World Journal of Gastroenterology

Submit a Manuscript: https://www.f6publishing.com

World J Gastroenterol 2024 August 14; 30(30): 3584-3608

DOI: 10.3748/wjg.v30.i30.3584

ISSN 1007-9327 (print) ISSN 2219-2840 (online)

ORIGINAL ARTICLE

Basic Study

Fanlian Huazhuo Formula alleviates high-fat diet-induced non-alcoholic fatty liver disease by modulating autophagy and lipid synthesis signaling pathway

Meng-Yuan Niu, Geng-Ting Dong, Yi Li, Qing Luo, Liu Cao, Xi-Min Wang, Qi-Wen Wang, Yi-Ting Wang, Zhe Zhang, Xi-Wen Zhong, Wei-Bo Dai, Le-Yu Li

Specialty type: Gastroenterology and hepatology

Provenance and peer review: Unsolicited article; Externally peer reviewed.

Peer-review model: Single blind

Peer-review report's classification

Scientific Quality: Grade B, Grade B

Novelty: Grade B, Grade B

Creativity or Innovation: Grade B, Grade B

Scientific Significance: Grade B, Grade B

P-Reviewer: Cheng TH; de Ceglia M

Received: April 18, 2024

Revised: July 15, 2024

Accepted: July 22, 2024

Published online: August 14, 2024

Processing time: 113 Days and 0.7 Hours

Meng-Yuan Niu, Geng-Ting Dong, Yi Li, Qing Luo, Liu Cao, Xi-Min Wang, Qi-Wen Wang, Yi-Ting Wang, Zhe Zhang, Xi-Wen Zhong, Wei-Bo Dai, Pharmacology Laboratory, Zhongshan Hospital of Traditional Chinese Medicine Affiliated to Guangzhou University of Traditional Chinese Medicine, Zhongshan 528400, Guangdong Province, China

Le-Yu Li, Department of Endocrinology, Zhongshan Hospital of Traditional Chinese Medicine Affiliated to Guangzhou University of Traditional Chinese Medicine, Zhongshan 528400, Guangdong Province, China

Co-first authors: Meng-Yuan Niu and Geng-Ting Dong.

Co-corresponding authors: Wei-Bo Dai and Le-Yu Li.

Corresponding author: Le-Yu Li, MS, Chief Physician, Department of Endocrinology, Zhongshan Hospital of Traditional Chinese Medicine Affiliated to Guangzhou University of Traditional Chinese Medicine, No. 3 Kangxin Road, West District, Zhongshan 528400, Guangdong Province, China. lileyu@zsszyy.net

Abstract

BACKGROUND

Fanlian Huazhuo Formula (FLHZF) has the functions of invigorating spleen and resolving phlegm, clearing heat and purging turbidity. It has been identified to have therapeutic effects on type 2 diabetes mellitus (T2DM) in clinical application. Non-alcoholic fatty liver disease (NAFLD) is frequently diagnosed in patients with T2DM. However, the therapeutic potential of FLHZF on NAFLD and the underlying mechanisms need further investigation.

AIM

To elucidate the effects of FLHZF on NAFLD and explore the underlying hepato-protective mechanisms *in vivo* and *in vitro*.

METHODS

HepG2 cells were treated with free fatty acid for 24 hours to induce lipid accumulation cell model. Subsequently, experiments were conducted with the different concentrations of freeze-dried powder of FLHZF for 24 hours. *C57BL/6* mice were

fed a high-fat diet for 8-week to establish a mouse model of NAFLD, and then treated with the different concentrations of FLHZF for 10 weeks.

RESULTS

FLHZF had therapeutic potential against lipid accumulation and abnormal changes in biochemical indicators *in vivo* and *in vitro*. Further experiments verified that FLHZF alleviated abnormal lipid metabolism might by reducing oxidative stress, regulating the AMPKα/SREBP-1C signaling pathway, activating autophagy, and inhibiting hepatocyte apoptosis.

CONCLUSION

FLHZF alleviates abnormal lipid metabolism in NAFLD models by regulating reactive oxygen species, autophagy, apoptosis, and lipid synthesis signaling pathways, indicating its potential for clinical application in NAFLD.

Key Words: Fanlian Huazhuo Formula; Nonalcoholic fatty liver disease; Autophagy; Apoptosis; AMPKα/SREBP-1C signal pathway; Oxidative stress

Core Tip: Fanlian Huazhuo Formula (FLHZF) has traditionally been used for treating type 2 diabetes mellitus. It has shown significant potential in treating non-alcoholic fatty liver disease (NAFLD) based on experimental research conducted *in vivo* and *in vitro*. Studies suggest that FLHZF may improve NAFLD by reducing oxidative stress, activating cellular autophagy, and regulating lipid metabolism signaling pathways. These findings provide new insights into the mechanism of action of FLHZF, and offer a theoretical basis for its application in the clinical treatment of NAFLD, potentially expanding its scope of use.

Citation: Niu MY, Dong GT, Li Y, Luo Q, Cao L, Wang XM, Wang QW, Wang YT, Zhang Z, Zhong XW, Dai WB, Li LY. Fanlian Huazhuo Formula alleviates high-fat diet-induced non-alcoholic fatty liver disease by modulating autophagy and lipid synthesis signaling pathway. *World J Gastroenterol* 2024; 30(30): 3584-3608
URL: https://www.wjgnet.com/1007-9327/full/v30/i30/3584.htm
DOI: https://dx.doi.org/10.3748/wjg.v30.i30.3584

INTRODUCTION

Non-alcoholic fatty liver disease (NAFLD) is a prevalent disease, affecting approximately 25.2% of the global population [1]. It is primarily characterized by disruptions in lipid metabolism due to the abnormal accumulation of fat in the liver [2]. These disturbances are caused by factors such as non-alcoholic substances and specific liver injuries[3]. The association between obesity and type 2 diabetes mellitus (T2DM) is well-established[4]. In the progression of T2DM, there is an increase in lipid bodies and carbohydrate synthesis fluxes in the liver, leading to lipid metabolism disorders[4]. Therefore, it is crucial to regulate lipid metabolism disorders for the treatment of NAFLD and related diseases[5]. Clinical drugs commonly used to treat NAFLD include insulin sensitizers, fibrates and statins[6]. However, these drugs often cause gastrointestinal reactions, osteoporosis, edema and other adverse effects[7]. Currently, there are no specific drugs approved by the United States Food and Drug Administration for treatment of NAFLD[8]. Hence, the development of new drugs to regulate lipid metabolism disorders and treat NAFLD is of importance.

At present, the widely recognized pathogenesis of NAFLD is known as the "second strike" theory[9]. The initial stage, also referred to as steatosis, is caused by the abnormal accumulation of lipids in liver cells and disruption of lipid metabolism due to insulin resistance[10,11]. The "second strike" involves the inflammatory response, oxidative stress, and apoptosis triggered by the accumulation of fat, which worsens NAFLD[12]. Normally, the liver maintains a dynamic balance between the absorption, synthesis, breakdown, and elimination of lipid, which is closely linked to lipid levels in the liver[13]. However, when the body consumes or produces excessive high-calorie food, surpassing the liver's capacity to break down or remove lipid, abnormal lipid accumulation occurs in liver cells, leading to disruption in fat metabolism [14]. Ingestion of high-fat diet (HFD) results in the build-up of lipotoxic substances, such as excess free fatty acids (FFAs), triglycerides (TGs), palmitic acid[15]. The accumulation of lipotoxic substances leads to the generation of reactive oxygen species (ROS), causing oxidative damage and promoting the production of lipid peroxide[16]. These substances also inhibit the production of antioxidant enzymes and induce apoptosis[17]. Additionally, lipotoxic substances also activate the AMPKα signaling pathway, which affects lipid metabolism[16,18]. Reduced AMPKα activity is strongly associated with the development of metabolic diseases such as obesity, diabetes and NAFLD[19,20]. In the treatment of NAFLD and the regulation of lipid metabolic disorder, increasing the activity of AMPKα can down-regulate the expression of adipogenic genes, thereby inhibiting the synthesis of fatty acids and cholesterol[21]. This inhibition of fat synthesis promotes fat oxidation and decomposition, and helps regulate lipid metabolism disorders[22,23]. AMPKα can also activate autophagy, a process that helps maintain body homeostasis by removing misfolded proteins and damaged

organelles, thus controlling cell quality[24]. In addition, insulin resistance, excess TG and FFAs, endoplasmic reticulum (ER) stress and oxidative stress all lead to decreased autophagy in the pathogenesis of NAFLD[25]. Currently, autophagy is considered as another pathway that can regulate lipid metabolism in hepatocytes by preventing hepatotoxicity and steatosis[26]. Therefore, regulating the signaling pathways associated with autophagy and lipid synthesis has potential for the treatment of NAFLD.

Nowadays, the application of traditional Chinese medicines is more extensive, and its curative effect is gradually gaining recognition worldwide. Some Chinese medicines have been shown to have the effects of anti-inflammatory, antioxidant, anti-apoptotic, regulatory ER stress and autophagy[27,28].

Fanlian Huazhuo Formula (FLHZF), also called Fufang Fanshiliu Formula, is a combination of traditional Chinese medicines including *Psidium guajava* L. (Fanshiliuye), *Ficus simplicissima* Lour. (Wuzhimaotao), *Morus alba* L. (Sangye), *Codonopsis pilosula* Nannf. (Dangshen), *Coptis chinensis* Franch. (Huanglian), *Atractylodes* (Cangzhu), *Crataegus pinnatifda* Bunge. (Shanzha), *Euonymus alatus* (Thunb.) Siebold (Guijianyu), *Monascus purpureus* Went. (Hongqu) and *Rhizoma Zingiberis* (Ganjiang in Chinese, derived from the dry rhizome of *Zingiber officinale* Rosc.). Previous studies have shown that *Psidium guajava* L. can lower the level of TG[28,29]. The extracts of *Ficus simplicissima* Lour. effectively reduce the levels of liver injury indexes in NAFLD mice[30]. *Morus alba* L. and its active ingredients have been shown to regulate lipid levels disorders and promote lipolysis[31]. The extract of *Codonopsis pilosula* Nannf. and *Euonymus alatus* (Thunb.) Siebold have the function of regulating the disorder of lipid metabolism disorder[32,33]. The Chinese herbal compound and the main active ingredients of *Coptis chinensis* Franch. can reduce blood glucose and lipid levels[34,35]. The *Coptis chinensis* Franch-*Monascus purpureus* Went. herb pair exhibits improvement in lipid metabolism[36]. *Rhizoma Zingiberis* causes a marked decrease in body weight and inflammation as well as amelioration of insulin resistance[37]. *Crataegus pinnatifda* Bunge. significantly reduces body weight and fat weight and regulates lipid indexes [including TG and total cholesterol (TC)] in obesity or dyslipidemia[38].

Clinical and experimental studies have shown that FLHZF regulates the structure of intestinal flora, inhibits the expression of pro-inflammatory factors, and alleviates symptoms of T2DM in rats[39]. In addition, FLHZF has been found to regulate PI3K/AKT, JAK/STAT and ER stress signaling pathways, thereby mitigating abnormal changes in blood glucose and lipid levels in mice with T2DM[40]. Previous studies have focused on the mechanisms of FLHZF in regulating lipid metabolism disorders specifically in T2DM, and there is a lack of studies investigating targeted improvement of lipid-metabolism-related diseases by FLHZF. Therefore, this study aimed to establish cellular and animal models of NAFLD to explore the potential mechanisms of FLHZF in regulating lipid metabolism disorders, with the goal of expanding the application range of FLHZF.

MATERIALS AND METHODS

Chemicals and reagents

Pancreatic enzyme (GX25200) was purchased from Guangzhou Jingxin Biotechnology Co. Ltd. (Guangzhou, China). TG assay kit (A110-1-1), TC assay kit (A111-1-1), low-density lipoprotein cholesterol (LDL-C) assay kit (A113-1-1), high-density lipoprotein cholesterol (HDL-C) assay kit (A112-1-1), aspartate aminotransferase (AST) assay kit (C010-2-1), alanine aminotransferase (ALT) assay kit (C009-2-1) and superoxide dismutase (SOD) (A001-3-2) assay kit (WST-1 method) were purchased from Nanjing Jiancheng Bioengineering Research Institute (Nanjing, China). Lipid peroxidation malondialdehyde (MDA) assay kit (S0131S) and cellular glutathione peroxidase (GSH-Px) assay kit with DTNB (S0057S) were purchased from Beyotime Biotechnology (Shanghai, China). ROS assay kit (S0033M), RIPA lysis buffer (P0013B) protease and phosphatase inhibitor cocktail (general use, 50 ×) (P1046) were purchased from Beyotime Biotechnology (Shanghai, China). Cell counting kit-8 (CCK8) (MA0218-3), DMEM (MA0212-Jun-021) and superior fetal bovine serum (FBS) (PWL001) were purchased from Meilun Biology-Dalian Meilun Biotechnology Co. Ltd. (Dalian, China). Fatty-acid-free bovine serum albumin V (BSA-V) (A8850-5G) was purchased from Solarbio (Beijing, China). Sodium palmitate (PA) (P9767), oleic acid (OA) (O1383-1G) and Oil Red O solution (1320-06-5) were purchased from Sigma-Aldrich (Cincinnati, OH, United States). TUNEL (Fluorescence) detection kit (GDP1042) was purchased from Wuhan Servicebio Technology Co. Ltd. (Wuhan, China). ACC1 antibody (AF6421), SREBP-1C antibody (AF6283), Bcl-2 antibody (AF6139), and β-actin antibody (AF7018) were purchased from Affinity Biosciences (Jangsu, China). AMPKα antibody (2532), p-AMPKα antibody (50081), LC3A/B antibody (12741), FASN antibody (3180), Bcl-2-associated X protein (BAX) antibody (2772), and cleaved caspase-3 antibody (9661) were purchased from Cell Signaling Technology (Danvers, MA, United States). Fenofibrate fenofibrate (FNBT) (Product No: 442973S) was purchased from Abbott Trading Co. Ltd. (Chicago, United States). Multiskan™ FC Microplate Reader (51119180ET) and TRIzol™ reagent (15596026) were purchased from Thermo Fisher Scientific (Waltham, MA, United States). Chemiluminescence imaging system (Product No: 10044275) was purchased from Bio-Rad Laboratories (Hercules, CA, United States). Affinity™ ECL kit (femtogram) (KF8003) was purchased from Affinity Biosciences. HFD (D12492) (consisting of 26.17% casein, 0.39% L-cystine, 16.35% maltodextrin.9.00% sucrose, 6.54% cellulose, 3.27% soybean oil, 32.06% lard, 4.58% mineral ain-93, 1.31% vitamin ain-93, 0.33% choline chloride, 1.0% cholesterol, 0.15% bile salt) was provided by Guangdong Experimental Animal Center (Guangdong, Chain).

Drugs preparation

Composition, specifications and sources of FLHZF: *Psidium guajava* L. (Fanshiliuye, C22103062, 30 g), *Ficus simplicissima* Lour (Wuzhimaotao, C22108042, 20 g), *Morus alba* L. (Sangye, C22110151, 15 g), *Codonopsis pilosula* Nannf. (Dangshen, C12108207, 30 g), *Coptis chinensis* Franch. (Huanglian, C22105098, 10 g), *Atractylodes lancea* (Thunb.) DC. (Cangzhu,

C22105060, 15 g), and *Crataegus pinnatifda* Bunge. (Shanzha, C22106013, 15 g) were purchased from Sinopharm Feng Liaoxing (Foshan) Herbal Pieces Co., Ltd (Guangdong, China), *Euonymus alatus* (Thunb.) Siebold. (Guijianyu, 200601, 15 g) and *Monascus purpureus* Went. (Hongqu, 210901, 15 g) were purchased from Zhixin Chinese pharmaceutical Co., Ltd (Guangdong, China), *Rhizoma Zingiberis* (Ganjiang, 210801, 10 g) was purchased from Bencaotang Chinese Pharmaceutical Co., Ltd. (Guangxi, China). The methods of preparation and administration of FLHZF were all as described previously[41,42]. In the preliminary studies, the chemical compositions of FLHZF were identified by quadrupole-time of flight-mass spectrometry, and the quality of FLHZF was controlled by the recorded chromatographic peaks of HPLC[39, 40]. FFA solution was prepared by conjugating OA (40 mmol/L) and PA (20 mmol/L) with 400 g/L fatty-acid-free BSA-V in a full medium. The final FFA concentration was 0.15 mmol/L.

Animal study

A total of 40 SPF-grade *C57BL/6J* mice (male, 6-8 weeks, 18-20 g) were purchased from the Experimental Animal Center of Guangdong Province (No. 44007200107205). All the mice were raised under SPF condition with 12 hours dark/light cycle and had free access to sterile water and diet. The temperature of the environment was 22-24 °C and the humidity was 50%-52%. The animal experiment protocol was reviewed and approved by the Experimental Animal Ethics Committee of Zhongshan Hospital of Traditional Chinese Medicine, and conformed to the principles of animal protection. The study adhered to the principles of animal protection, animal welfare, and ethics, as well as the relevant provisions of the state on the ethical welfare of experimental animals (Approval number: AWC-2022042). At the end of the experiment, all mice were anesthetized with isoflurane (inhalation anesthesia, 1.5% concentration, 2-3 minutes) and the animal tissues were collected.

After 1 week of adaptive feeding, the mice were randomly divided into two groups: Normal control (NC) group, consisting of 8 weeks that were fed with a normal diet, and the HFD group, consisting of 32 mice that were fed with HFD for 8 weeks. The mice in the HFD group, which showed changes in clinically relevant serum indicators (TG, TC, LDL-C, HDL-C, AST and ALT) associated with NAFLD were considered to be NAFLD model mice. The NAFLD model mice were randomly divided into four groups randomly: Model (MOD) group, the FNBT group, low dose of FLHZF (FLHZF-L) group and high dose of FLHZF (FLHZF-H) group. The low dose of FLHZF administered per gram of mouse per day is calculated as = (175 g/d)/70 kg × 9.1 = 22.75 g/(kg/d) and the high dose was calculated as = (175/d)/70 kg × 9.1 × 2 = 45.5 g/(kg/d); 175 g is the daily dosage for an adult, 70 kg is the average weight of an adult, and 9.1 is the coefficient. In addition to the above feeding methods, mice in the fenofibrate, FLHZF-L and FLHZF-H groups were administered the corresponding drug once daily for 10 weeks. The body weight of all mice was monitored throughout the experiment. Following the final treatment, all mice were anesthetized with isoflurane and their blood, livers, and fat were collected. The fat index in mice was calculated by determining the ratio of the fat tissue weight to the body weight. The specific formula for the fat index was: Fat index = weight of fat tissue (mg)/body weight of mice (g). The liver index was ascertained by dividing the liver weight by the body weight of the mice. The formula for calculating the liver index was: Liver index = weight of liver tissue (mg)/body weight of mice (g).

Cell culture

HepG2 cells were purchased from Cell Bank of Shanghai Institute of Cell Biology, Chinese Academy of Sciences. Cells were cultured in DMEM containing 100 mL/L FBS and 10 mL/L penicillin-streptomycin (PS) and maintained in an incubator with 50 mL/L CO_2 at 37 °C.

Cell viability assay

HepG2 cells were inoculated into a 96-well plate with an initial density of 10^5 cells per well. After adhering to the walls, the cells were cultured in an incubator for 4 hours. HepG2 cells were incubated with a solution containing 0.15 mmol FFA, which consisted of fatty acid-free BSA-conjugated OA and PA in a 2:1 ratio or vehicle for 24 hours[41,43]. Following FFA stimulation, freeze-dried powder of FLHZF (25, 50, 100 or 200 μg/mL), which was diluted with full medium (DMEM containing 100 mL/L FBS and 10 mL/L PS), was added to the corresponding wells and cultured for an additional 24 hours. Finally, the cell supernatant was removed, a 100 mL/L CCK8 solution (diluted with complete medium) was added to the 96-well plate and incubated for 2 hours. The absorbance of the plate was measured at 450 nm using the VICTOR Nivo (HH35000500, Perkin Elmer, MA, United States).

Serum biochemical analysis

Concentration of TG, TC, LDL-C, HDL-C, AST, ALT, SOD, GSH-Px and MDA were evaluated by commercial detection kits.

Hematoxylin and eosin staining

Liver tissue sections were dissected and fixed in the tissue fixative solution. The tissues were dehydrated and embedded in paraffin. The tissues were stained with hematoxylin solution for 3-5 minutes, followed by staining with eosin for 15 seconds. Images was captured through a microscope at 200 × magnification. Quantitative analysis of hematoxylin and eosin (HE) staining was based on the NAFLD Activity Score (NAS)[44].

Immunohistochemistry

Liver tissue sections were dewaxed using water and then incubated with hydrogen peroxide (H_2O_2). After washing the sections once or twice with phosphate-buffered saline (PBS), they were cooled during microwave repair. Goat serum was applied to block the sections for 20 minutes. The negative control was replaced with PBS, and the sections were treated

overnight at 4 °C. The secondary antibody was added and incubated at room temperature for 20 minutes. This was followed by diaminobenzidine color development, re-staining with hematoxylin, and sealing with neutral gum. Images were captured under an optical microscope, and quantitative analysis was performed using ImageJ.

Oil Red O staining

Frozen liver tissues were cut into 15-μm slices. After fixation and oil red staining of slices, the background differentiation, hematoxylin staining and sealing were also used. The images were captured using a fluorescence microscope (ECLIPSE Ti2-A; Nikon, Tokyo, Japan) at 400 × magnification. Intracellular lipid droplets of HePG2 cells were observed by Oil Red O staining. According to the instruction, the prepared Oil Red O solution was used to stain for 20 minutes in a dark environment. After washing with 600 mL/L isopropyl alcohol, the red-stained lipid droplets were observed by fluorescence Microscopy at 400´ magnification Quantitative analysis of the images was performed using ImageJ.

ROS detection

Dichloro-fluorescein Diacetate (DCFH-DA) was diluted in serum-free medium at a ratio of 1:1000 to achieve a final concentration of 10 μmol/L. The cells were incubated with diluted DCFH-DA at 37 °C for 20 minutes. After incubation, the cells were washed three times with serum-free cell culture solution to ensure complete removal of DCFH-DA that did not enter the cells. The ROS level was measured by flow cytometry (A00-1-1102; Beckman Coulter, Brea, CA, United States).

Western blotting

Total proteins of livers and HepG2 cells were extracted using prechilled RIPA buffer containing protease and phosphatase inhibitors. An equal amount of protein sample was separated by SDS-PAGE and transferred to polyvinylidene fluoride membranes. The membranes were blocked with 50 mL/L non-fat milk in PBS containing 1 mL/L Tween-20 (PBST) at room temperature for 2 hours. For protein detection, the membranes were incubated with corresponding primary antibodies overnight at 4 °C, washed with PBST three times, and incubated with secondary horseradish peroxidase-conjugated antibody at room temperature for 2 hours. The membranes were washed three times and protein bands were visualized using Affinity™ ECL kit (femtogram) under a chemiluminescence imaging system. A densitometric analysis of protein expression was performed using Image J (National Institutes of Health, Bethesda, MD, United States).

Real-time quantitative polymerase chain reaction

To test mRNA expression in mouse liver tissue and HepG2 cells, total RNA was extracted by TRIzol reagent. The cDNA synthesis was performed using Prime Script TM RT Master Mix (RR036A) purchased from Takara Biomedical Technology (Beijing) Co. Ltd. (Takara, Japan). Real-time quantitative polymerase chain reaction (RT-qPCR) was performed using TB Green® Premix Ex Taq™ (Tli RNaseH Plus) (RR420A; Takara Biomedical Technology). The mRNA levels were determined by calculating the ratio of the signal intensity for each gene relative to that of β-actin. The primer information is shown in Table 1.

Terminal deoxynucleotidyl transferase-mediated dUTP nick-end labeling

To detect apoptosis of liver in mouse, TUNEL (fluorescence) detection kit was used according to manufacturer's instructions. Fluorescence signals were detected with the Fluorescence Microscope. Finally, quantitative analysis of the images was performed using ImageJ.

Statistical analysis

SPSS version 25.0 was used for data analysis. All statistical charts were created by GraphPad Prism version 9.0 (GraphPad, La Jolla, CA, United States). All results were presented as mean ± SE. One-way analysis of variance was used for normal data and Mann-Whitney *U* test was used for non-normal data. $P < 0.05$ was considered statistically significant.

RESULTS

FLHZF reduced lipid droplets deposition in HepG2 cells induced by FFA

To evaluate the therapeutic effect of FLHZF on NAFLD, we conducted *in vitro* experiments on HepG2 cells stimulated with FFA. The solvent group showed no significant effect on the cell viability of HepG2 cells, and the decrease of cell viability of HepG2 cells caused by FFA could be effectively improved by FLHZF (Figure 1A). Different concentrations of FLHZF had no effect on TG accumulation in HepG2 cells (Figure 1B). After treatment with FLHZF, there was a noticeable decrease in the percentage of areas positive for Oil Red O staining and TG content in HepG2 cells stimulated by FFA (Figure 1C-E). HepG2 cells stimulated by FFA exhibited a significant increase in red-stained lipids by Oil Red O staining and intracellular TG content. However, the red-stained lipids and TG in HepG2 cells induced by FFA were decreased significantly by treatment with FLHZF. These results indicated that FLHZF has the potential to reduce TG accumulation in HepG2 cells stimulated by FFA (Figure 1).

Table 1 The primer information

Gene name	Primer sequence (5' -3')	
Homo-AMPKα	Forward	5'-TTTGCGTGTACGAAGGAAGAATCC-3'
	Reverse	5'-CTGTGGAGTAGCAGTCCCTGATTT-3'
Homo-β-actin	Forward	5'-GAGCACAGAGCCTCGCCTTT-3'
	Reverse	5'-ACATGCCGGAGCCGTTGTC-3'
Homo-SREBP-1C	Forward	5'-CTTAGAGCGAGCACTGAACTGTGTG-3'
	Reverse	5'-CTGGAACTGATGGAGAAGCTGTAGG-3'
Homo-ACC1	Forward	5'-GGCCAGTGCTATGCTGAGATT-3'
	Reverse	5'-GTACACAGCCAGGGTCAAGAG-3'
Homo-FASN	Forward	5'-TGAGTGGGAAGGTGTACCAGT-3'
	Reverse	5'-CTGGAAATGAGGGCCGTAGTC-3'
Mus-AMPKα	Forward	5'-GTCCTGCTTGATGCACACATGAAT-3'
	Reverse	5'-ATGACTTCTGGTGCGGCATAATTG-3'
Mus-LC3A	Forward	5'-CTGCCTGTCCTGGATAAGACCAAG-3'
	Reverse	5'-ATAGATGTCAGCGATGGGTGTGG-3'
Mus-LC3B	Forward	5'-CCAAGATCCCAGTGATTATAGAGCGA-3'
	Reverse	5'-ACGTGGTCAGGCACCAGGAAC-3'
Mus-SREBP-1C	Forward	5'-GCTTGTACCCACTGGTAGAGCATA-3'
	Reverse	5'-CTGGGCTAGATTCCACCTTTCTGT-3'
Mus-ACC1	Forward	5'-GAAAATCCACAATGCCAACCCTGA-3'
	Reverse	5'-TCTTCCTCTGTCAGTTGCTTCTCC-3'
Mus-Bcl2	Forward	5'-GATTGTGGCCTTCTTTGAGTTCGG-3'
	Reverse	5'-GGTTCAGGTACTCAGTCATCCACA-3'
Mus-Bax	Forward	5'-CGAATTGGAGATGAACTGGACAGC-3'
	Reverse	5'-AGTTGAAGTTGCCATCAGCAAACA-3'
Mus-cleaved caspase-3	Forward	5'-TACCATGTTCCTTGAAATCTGCACC-3'
	Reverse	5'-AAGGCTTTGTTCATCTCGTACTTGG-3'
Mus-FASN	Forward	5'-CATCAGGCCACTATACTACCCAAGA-3'
	Reverse	5'-GAATAACTTGGAGTTCGGGTCTTCC-3'
Mus-β-actin	Forward	5'-CAACGGCTCCGGCATGTG-3'
	Reverse	5'-AGTCCTTCTGACCCATTCCCA-3'

The "Mus" presented in this table refers to the species "Mouse"; The "Homo" presented in this table refers to the species Human.

FLHZF alleviated lipid accumulation and liver injury in mice induced by HFD

To verify the regulatory effect of FLHZF on lipid accumulation and liver injury, an animal model of NAFLD was established by inducing *C57BL/6J* mice with HFD (Figure 2A). The MOD group exhibited symptoms of metabolic syndrome, including significantly increased body weight, liver index and fat index, compared with the NC group) (Figure 2B-E). However, FLHZF significantly improved the abnormal changes of body weight, weight gain, organ (liver) and fat (abdominal, genital) index of mice with NAFLD caused by HFD. However, in the improvement of brown fat index, only the mice in the FLHZF-L group had a significant effect. The appearance of the liver in the MOD group showed a tight and smooth capsule, blunt edges (Figure 2F). After treatment with FLHZF, the liver showed a reddish-brown color, soft and brittle texture, loose capsule, and returned to the appearance in the NC group.

Blood lipid levels in each group are shown in Figure 3A-D. Compared with the NC group, the serum lipid levels in the MOD group showed significant abnormalities: TG, TC and LDL-C were increased, and HDL-C was decreased. These changes were consistent with lipid metabolism disorder associated with NAFLD. FLHZF alleviated abnormal changes in blood lipid levels in mice with NAFLD by decreasing TG and LDL-C and increasing HDL-C. Levels of AST and ALT

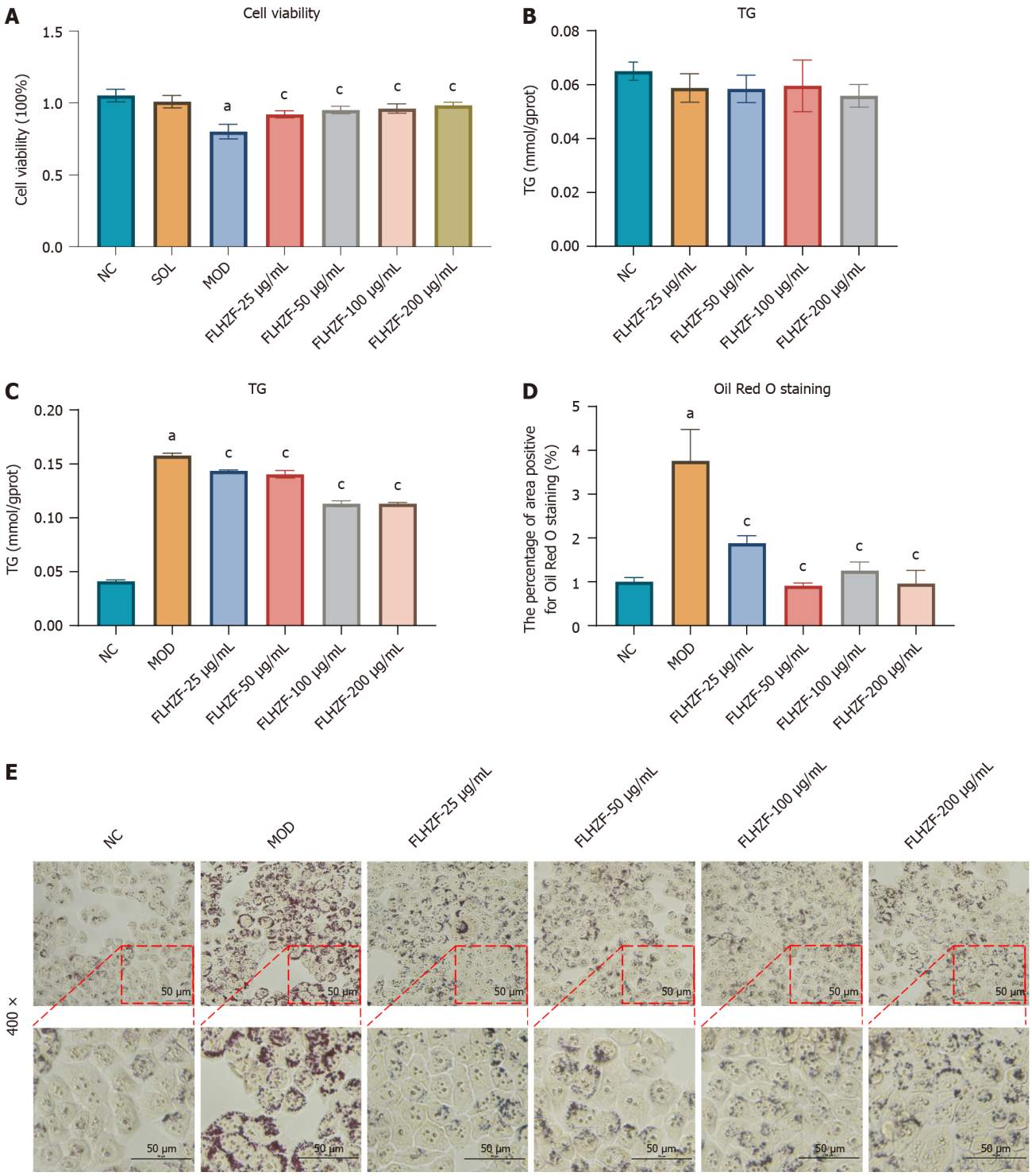

Figure 1 Fanlian Huazhuo Formula group reduced lipid droplets deposition in HepG2 cells induced by free fatty acid. A: Cell viability with Fanlian Huazhuo Formula group (FLHZF) treatment in free fatty acids (FFAs)-induced HepG2 cells tested by cell counting kit-8 (n = 3); B: Cell triglyceride (TG) content without or with FLHZF treatment in HepG2 cells (n = 3); C: Cell TG content with FLHZF treatment in FFA-induced HepG2 cells (n = 3); D: Percentage of area positive for Oil Red O staining in HepG2 cells (n = 3); E: Representative images of FFA-induced HepG2 cells of Oil Red O staining, magnification 400 ×. Data are presented as mean ± SE. $^{a}P < 0.05$ *vs* NC group, $^{c}P < 0.05$ *vs* MOD group. NC: Negative control group; SOL: Solvent group MOD: Model group; FLHZF: Fanlian Huazhuo Formula group; TG: Triglyceride.

were significantly increased in the MOD group (Figure 3E and F). FLHZF significantly reduced the levels of AST and ALT. H&E staining showed severe liver injury in the MOD group (Figure 3G). Treatment with FLHZF relieved liver injury induced by HFD. Oil Red O staining revealed lipid accumulation in the liver. Compared with the NC group (Figure 3H), Oil Red O staining in the MOD group showed severe steatosis and was characterized by lipid droplet formation. FLHZF treatment reduced accumulation of lipid drops in liver tissue. After FLHZF treatment, quantitative analysis of NAS (Figure 3I) and Oil Red O staining (Figure 3J) in the livers of mice showed a significant decrease. These results suggested that FLHZF improved lipid metabolism disorder and liver injury in mice with NAFLD caused by HFD.

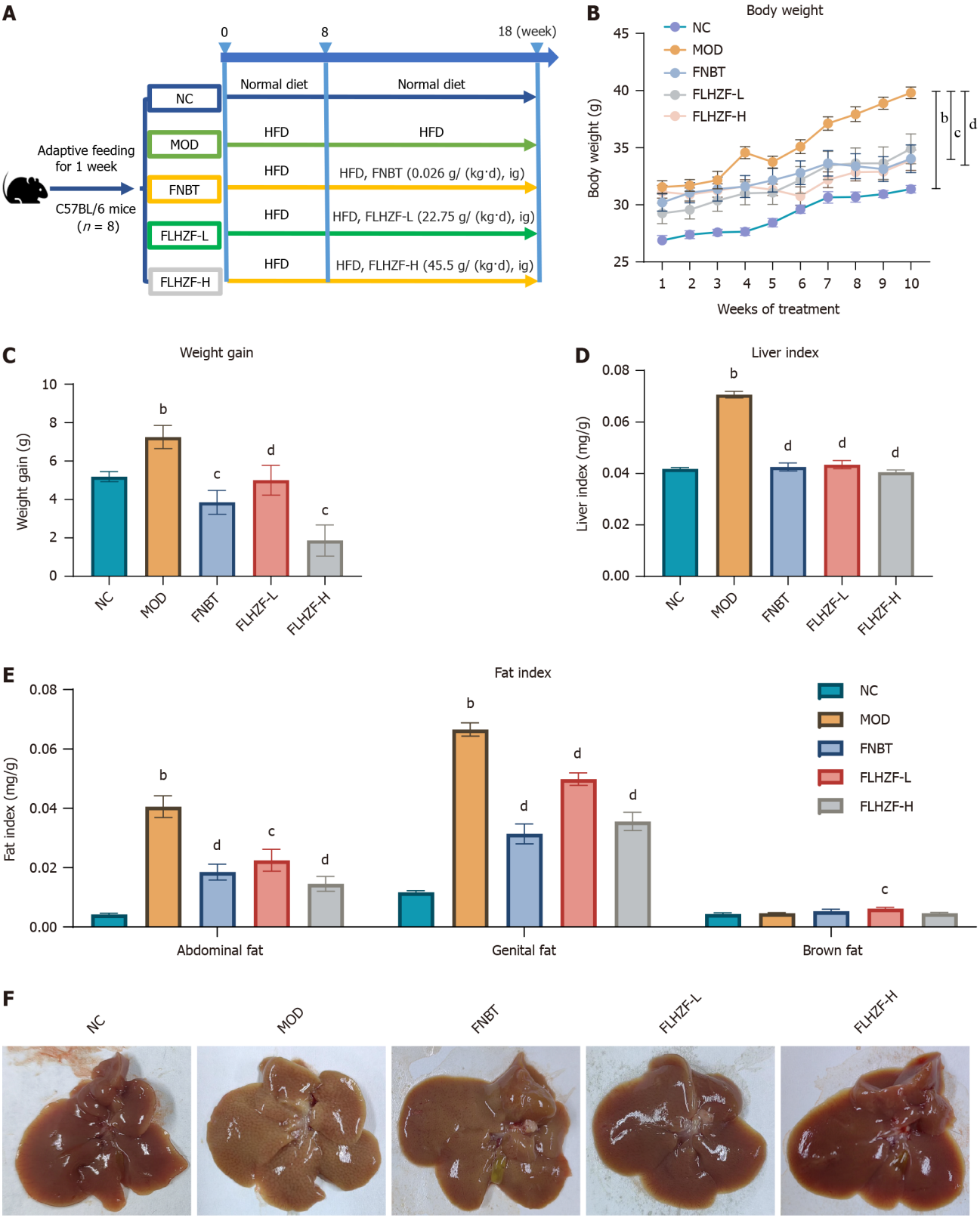

Figure 2 Effects of Fanlian Huazhuo Formula group on symptoms associated with nonalcoholic fatty liver disease mice. A: Flow chart of animal experiment protocol; B: Body weight of mice once a week for 10 weeks (n = 8); C: Weight change (pre-treatment weight minus post-treatment weight) of mice (n = 8); D: Liver index of nonalcoholic fatty liver disease (NAFLD) mice (n = 8); E: Fat index of NAFLD mice (n = 8); F: Representative images of livers after 10 weeks intervention in mice. Data are presented as mean ± SE. $^{b}P < 0.01$ *vs* NC group, $^{c}P < 0.05$ *vs* MOD group, $^{d}P < 0.01$ *vs* MOD group. NC: Negative control group; MOD: Model group; FNBT: Fenofibrate group; FLHZF-L: Low dose of Fanlian Huazhuo Formula group; FLHZF-H: High dose of Fanlian Huazhuo Formula group.

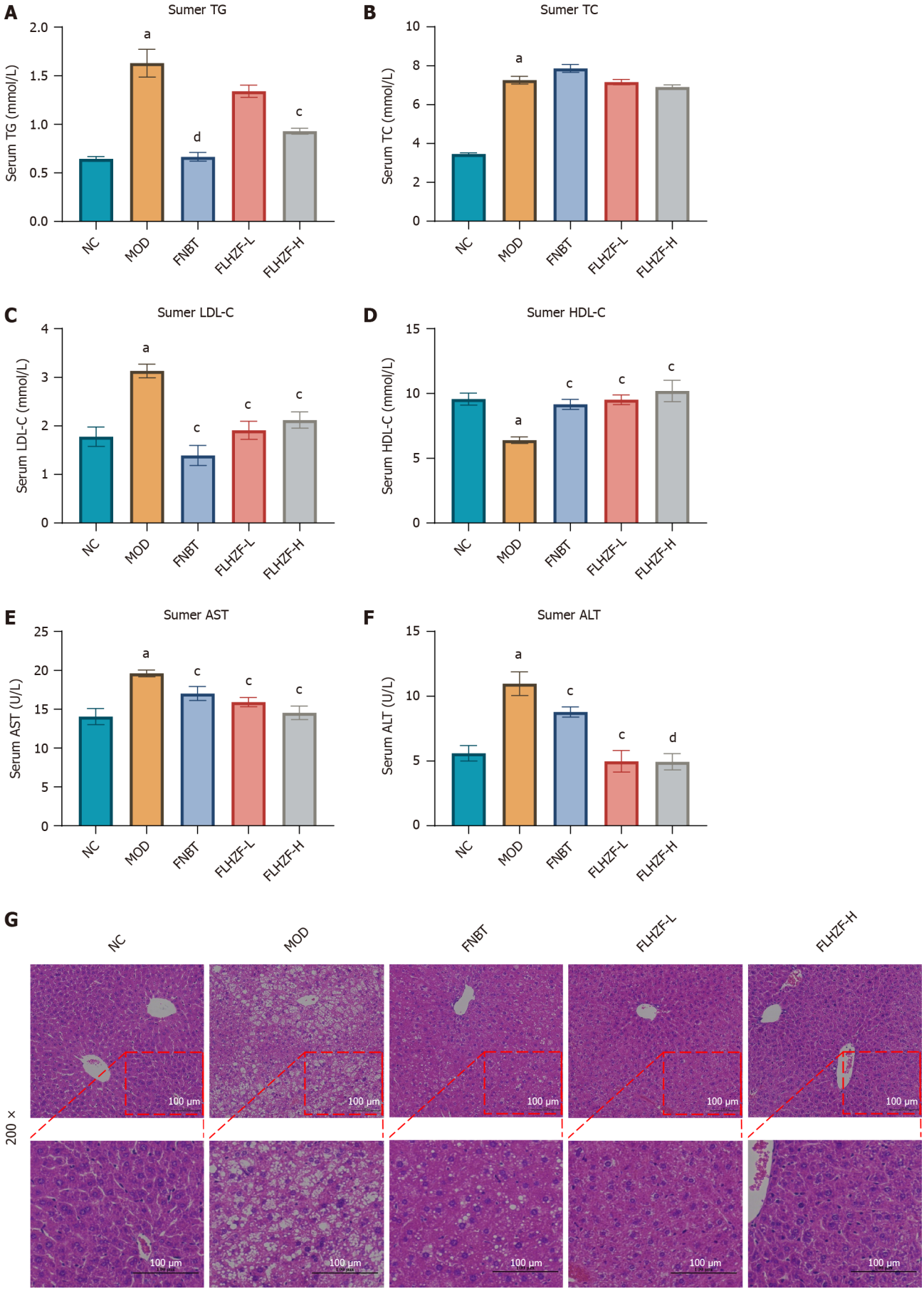
A
Sumer TG
Serum TG (mmol/L)
2.0
1.5
1.0
0.5
0.0
a
d
c
NC
MOD
FNBT
FLHZF-L
FLHZF-H
B
Sumer TC
Serum TC (mmol/L)
10
8
6
4
2
0
a
C
Sumer LDL-C
Serum LDL-C (mmol/L)
4
3
2
1
0
a
c
D
Sumer HDL-C
Serum HDL-C (mmol/L)
15
10
5
0
a
c
E
Sumer AST
Serum AST (U/L)
25
20
15
10
5
0
a
c
F
Sumer ALT
Serum ALT (U/L)
15
10
5
0
a
c
d
G
200 ×
100 μm

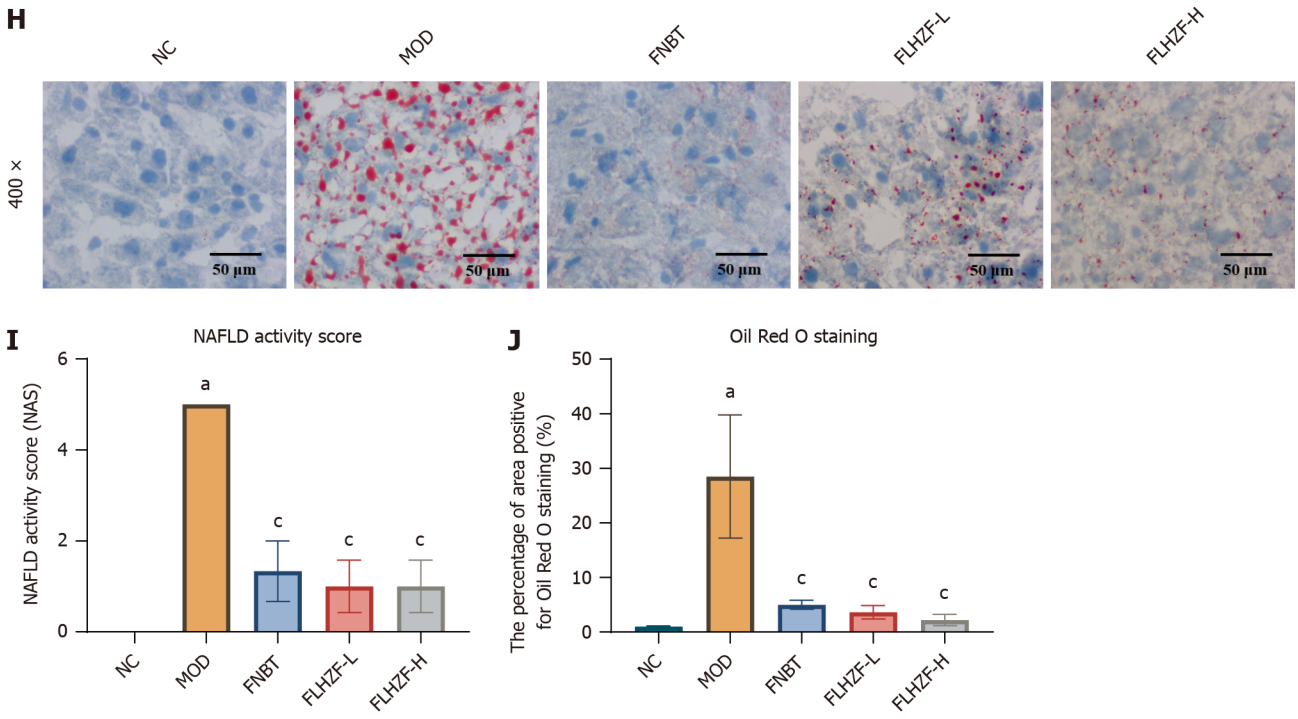

Figure 3 Effects of Fanlian Huazhuo Formula group on abnormal lipid levels and liver injuries in high-fat diet-induced mice. A: Serum levels of triglyceride in each group (n = 8); B: Serum levels of total cholesterol in each group (n = 8); C: Serum levels of low-density lipoprotein cholesterol in each group (n = 8); D: Serum levels of high-density lipoprotein cholesterol in each group (n = 8); E and F: Liver injury markers of aspartate aminotransferase and alanine aminotransferase in each group (n = 8); G: Representative images of livers with hematoxylin and eosin (HE) staining in each group, magnification 200 ×; H: Representative images of livers with Oil Red O staining in each group, magnification 400 ×; I: Nonalcoholic fatty liver disease Activity Score of HE staining (n = 3); J: Percentage of area positive for Oil Red O staining in liver tissue (n = 3). Data are presented as mean ± SE. $^{a}P < 0.05$ *vs* NC group, $^{c}P < 0.05$ *vs* MOD group, $^{d}P < 0.01$ *vs* MOD group. TG: Triglyceride; TC: Total cholesterol; LDL-C: Low-density lipoprotein cholesterol; HDL-C: High-density lipoprotein cholesterol; AST: Aspartate aminotransferase; ALT: Alanine aminotransferase; NC: Negative control group; NAFLD: Nonalcoholic fatty liver disease; MOD: Model group; FNBT: Fenofibrate group; FLHZF-L: Low dose of Fanlian Huazhuo Formula group; FLHZF-H: High dose of Fanlian Huazhuo Formula group.

FLHZF reduced oxidative damage in vivo and in vitro

In vitro studies showed that compared with the normal HepG2 cells group, the intracellular ROS level in the model group was significantly upregulated (Figure 4A and B). Intracellular ROS level was downregulated by treatment with FLHZF. *In vivo* experiments showed that FLHZF reduced the level of MDA and increased SOD and GSH-Px in the NAFLD mice (Figure 4C-E). These results indicated that the increase in ROS level caused by accumulation of lipid toxic substances could be reversed by FLHZF *in vivo* and *in vitro*.

FLHZF regulated lipid synthesis signaling pathway in vivo and in vitro

We examined changes in related proteins in TG synthesis and breakdown pathways in HepG2 cells and liver of mice. Protein and mRNA expression levels of AMPKα, ACC1, SREBP-1C and FASN in HepG2 cells and mouse liver showed that FLHZF significantly upregulated protein and mRNA expression levels of *AMPKα*, and significantly downregulated protein and mRNA expression levels of *ACC1*, *SREBP-1C* and *FASN* (Figures 5 and 6). FLHZF effectively increased protein expression of p-AMPKα and significantly reduced protein expression of p-ACC1 in the livers of NAFLD mice (Figure 6A). Immunohistochemistry (IHC) and quantitative analysis showed that protein expression of ACC1, p-ACC1 and FASN in liver in mice was significantly decreased after treatment with FLHZF (Figure 7). These results indicated that FLHZF may participate in the inhibition of TG synthesis by regulating the lipid synthesis signaling pathway in HepG2 cells stimulated by FFA and mice with NAFLD caused by HFD.

FLHZF regulated autophagy in mice induced by HFD

As described above, lipid peroxides can inhibit activation of AMPKα. Western blotting and RT-qPCR showed that FLHZF significantly increased levels of p-AMPKα, LC3A/B, *LC3A* and *LC3B* in mice with NAFLD (Figure 8A and B). IHC and quantitative analysis showed that compared with the NC group, protein expression of LC3A/B and p-AMPKα was significantly decreased in mouse liver in the model MOD group (Figure 8C and D). However, the protein expression levels of LC3A/B and p-AMPKα in the liver of mice was increased after treatment with FLHZF compared with in the model group. These results indicated that FLHZF improved the metabolic disorder of mice with NAFLD by regulating activation of autophagy.

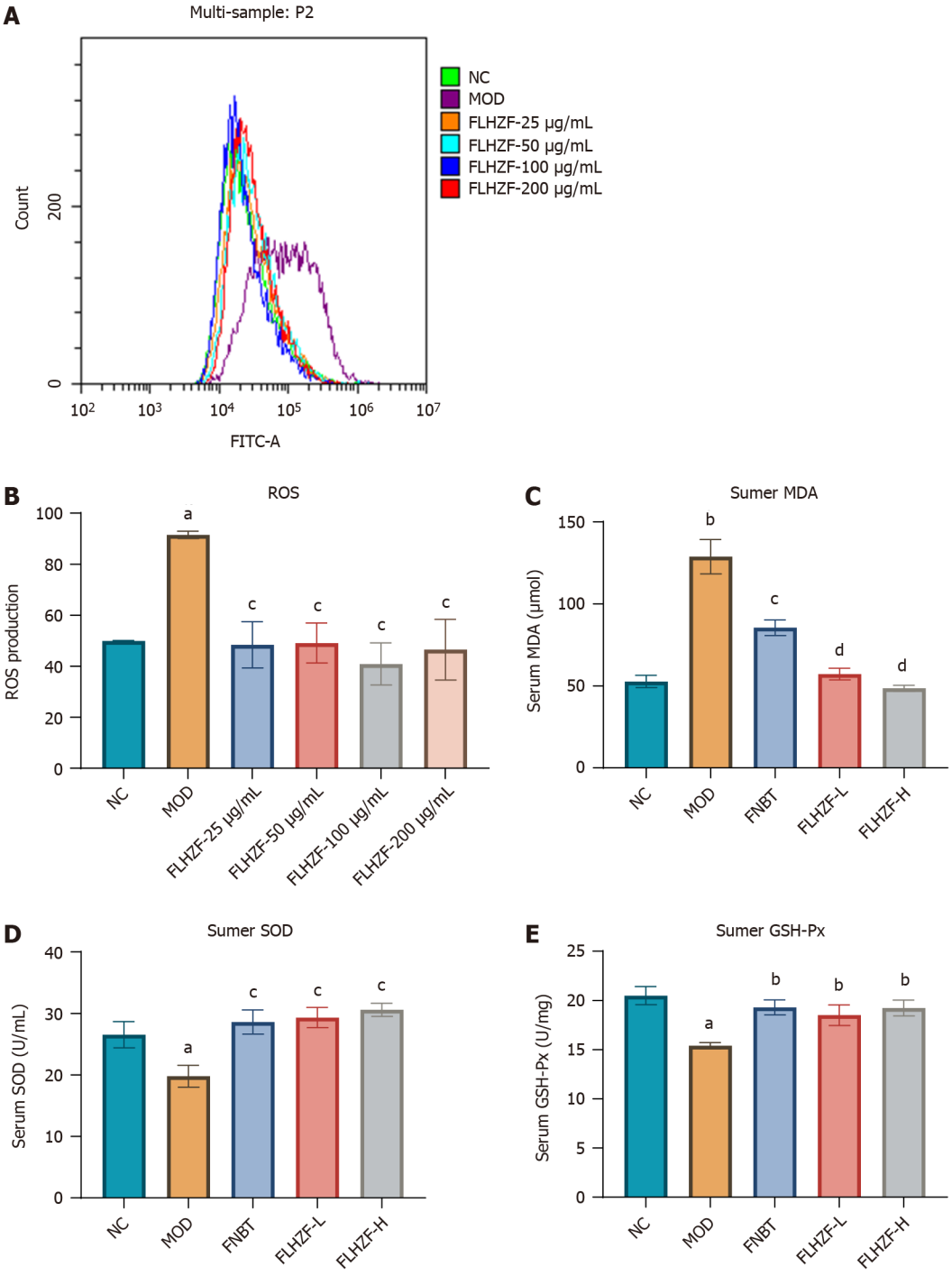

Figure 4 Fanlian Huazhuo Formula group reduced oxidative damage *in vivo* and *in vitro*. A: Cell reactive oxygen species (ROS) content with Fanlian Huazhuo Formula group treatment in HepG2 cells induced by free fatty acid (n = 3); B: Quantitative result of cell ROS content (n = 3); C: Serum levels of malondialdehyde (n = 8); D: Serum levels of superoxide dismutase (n = 8); E: Serum levels of glutathione peroxidase (n = 8). Data are presented as mean ± SE. ^{a}P < 0.05 *vs* NC group, ^{b}P < 0.01 *vs* NC group, ^{c}P < 0.05 *vs* MOD group, ^{d}P < 0.01 *vs* MOD group. ROS: Reactive oxygen species; MDA: Malondialdehyde; SOD: Superoxide dismutase: GSH-Px: Glutathione peroxidase; NC: Negative control group; MOD: Model group; FNBT: Fenofibrate group; FLHZF-L: Low dose of Fanlian Huazhuo Formula group; FLHZF-H: High dose of Fanlian Huazhuo Formula group.

FLHZF reduced apoptosis in mice induced by HFD

We investigated the effect of FLHZF on apoptosis-related molecular changes in mice with NAFLD. Protein and mRNA expression levels of Bax in liver were significantly downregulated by FLHZF, whereas the protein and mRNA levels of Bcl-2 were significantly increased by FLHZF (Figure 9A and B). IHC and quantitative analysis showed that FLHZF significantly reduced cleaved caspase-3 protein expression in mice with NAFLD caused by HFD (Figure 9C). TUNEL staining and quantitative analysis showed that FLHZF significantly decreased apoptotic cells stained green in mice with NAFLD caused by HFD (Figure 9D). The above results revealed that FLHZF reduced apoptosis by regulating expression of Bax, Bcl-2 and cleaved caspase-3 in mouse liver, thus FLHZF could play an important role in the treatment of NAFLD.

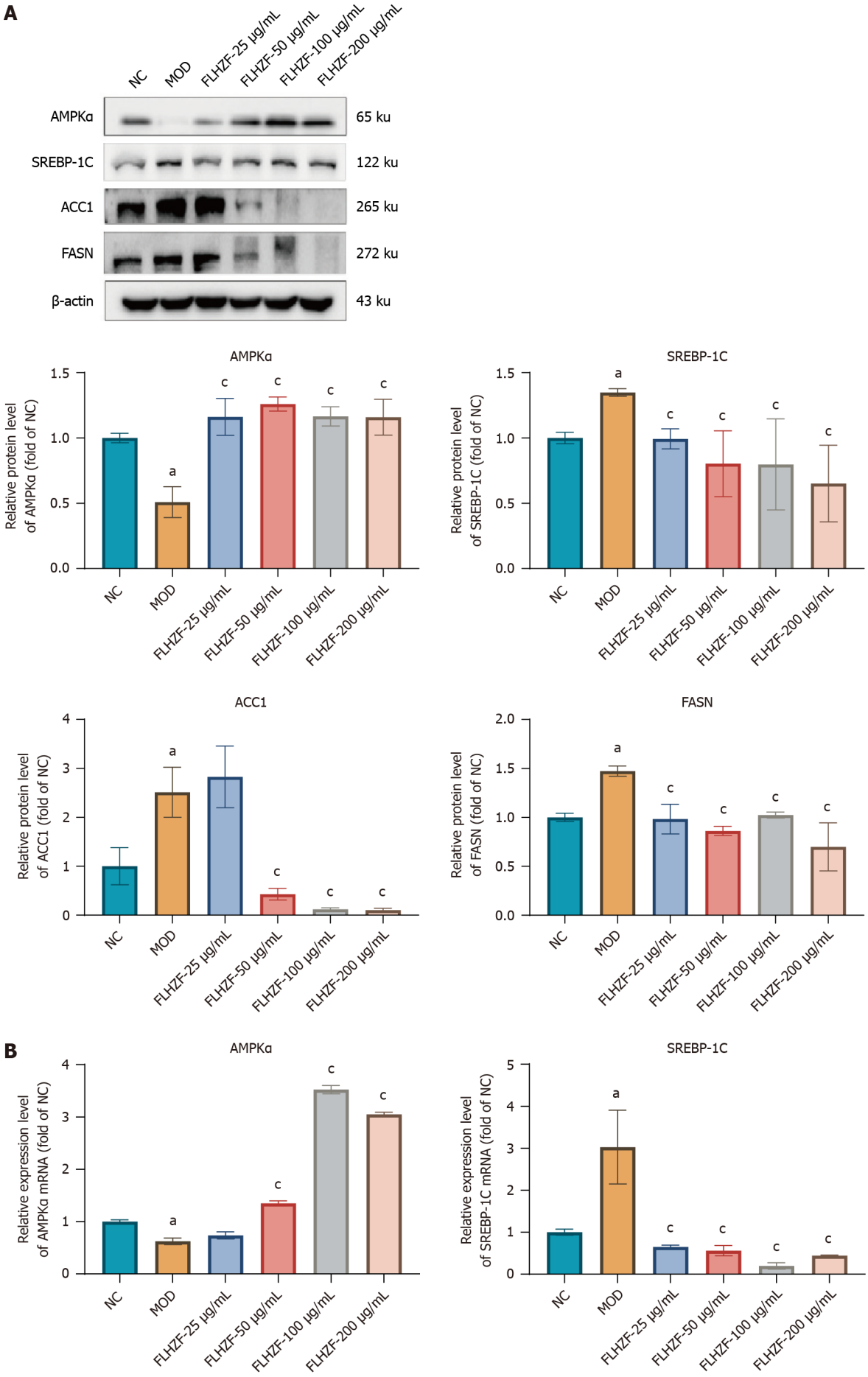
A
NC
MOD
FLHZF-25 μg/mL
FLHZF-50 μg/mL
FLHZF-100 μg/mL
FLHZF-200 μg/mL
AMPKα
SREBP-1C
ACC1
FASN
β-actin
65 ku
122 ku
265 ku
272 ku
43 ku
AMPKα
Relative protein level of AMPKα (fold of NC)
SREBP-1C
Relative protein level of SREBP-1C (fold of NC)
ACC1
Relative protein level of ACC1 (fold of NC)
FASN
Relative protein level of FASN (fold of NC)
B
AMPKα
Relative expression level of AMPKα mRNA (fold of NC)
SREBP-1C
Relative expression level of SREBP-1C mRNA (fold of NC)

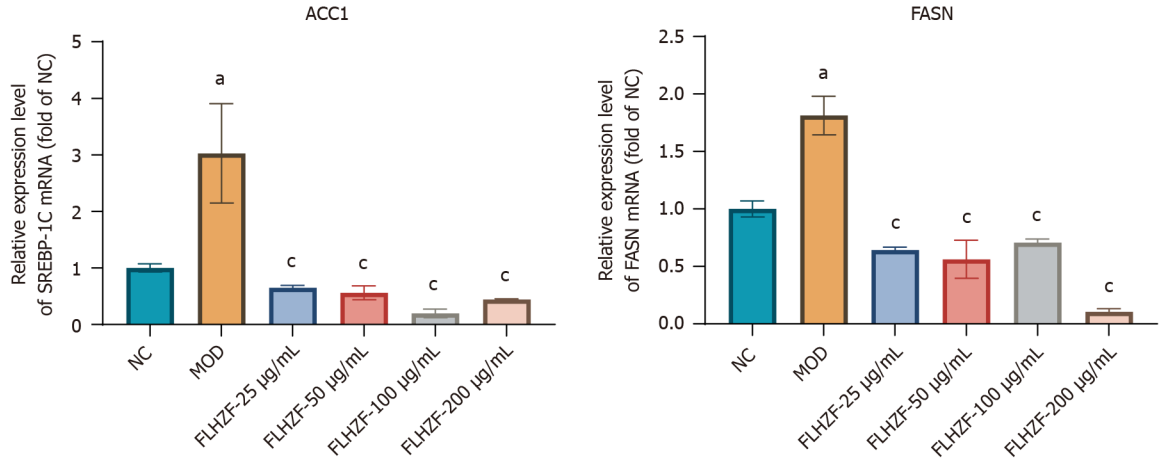

Figure 5 Fanlian Huazhuo Formula group regulated lipid synthesis signaling pathway *in vitro*. A: Protein expression levels of AMPKα, SREBP-1C, ACC1, FASN and β-actin in HepG2 cells induced by free fatty acid (*n* = 3); B: Relative mRNA expression levels of *AMPKα*, *SREBP-1C*, *ACC1* and *FASN* in HepG2 cells tested by real-time quantitative polymerase chain reaction (*n* = 3). Data are presented as mean ± SE. $^{a}P < 0.05$ *vs* NC group, $^{c}P < 0.05$ *vs* MOD group. NC: Negative control group; MOD: Model group; FLHZF: Fanlian Huazhuo Formula group.

DISCUSSION

HFD is currently the most common key factor causing NAFLD[45]. Long-term excessive intake of HFD can disrupt various lipid metabolic processes, such as excessive fatty acid synthesis, oxidative stress and mitochondrial β-oxidation leading to accumulation of lipotoxic substances[46]. Dysfunction of TG metabolism usually induces more severe cardiovascular disease[47,48]. Therefore, regulating TG metabolism is crucial for improving NAFLD and preventing other cardiovascular diseases. Normally, the body can regulate autophagy and the AMPKα/SREBP-1C signaling pathway to participate in the metabolism of TG[49]. However, in NAFLD, excessive intake of HFD causes the accumulation of lipotoxic substances, damaging mitochondrial function and resulting in a large number of ROS[50]. The increase in ROS inhibits autophagy and the AMPKα/SREBP-1C signaling pathway, which intensifies TG accumulation, liver cell apoptosis and injury, and aggravates the symptoms of NAFLD[51,52]. In the present, HFD-induced *C57BL/6J* mice and FFA-induced HePG2 cells were used as models of NAFLD *in vivo* and *in vitro*, respectively. Results revealed that FLHZF reduced the accumulation of lipotoxic substances and alleviated liver damage in NAFLD through activation of autophagy and lipid synthesis signaling pathways.

In vitro, FFA prepared by PA and OA was used to induce NAFLD cell models in HepG2 cells[53,54]. The abnormal increase of FFA concentration promoted the accumulation of lipid substances such as TG and TC, thereby contributing to the formation of NAFLD[54]. Shen *et al*[43] demonstrated that pterostilbene reduced lipid accumulation in HepG2 cells induced by OA and PA, and alleviated lipid accumulation in NAFLD by activating AMPKα activity and promoting expression of SREBP-1C. Li *et al*[41] showed that sodium tanshinone IIA sulfonate significantly inhibited lipid accumulation in HepG2 cells treated with OA and PA. In the present study, cell viability and intracellular TG content were measured to demonstrate that FLHZF has the potential to improve the decrease in cell viability and increase in TG accumulation caused by FFA. Oil Red O staining further demonstrated that FLHZF regulated lipid metabolic disorder in HepG2 cells stimulated by FFA. However, it remained unclear whether FLHZF could improve lipid accumulation in NAFLD mice.

Therefore, we used HFD to induce NAFLD in mice, which has been widely used as an animal model for studying NAFLD due to its similarities to the human disease[55]. Tovar *et al*[56] substantiated that linoleoylethanolamide, without reducing food intake, activates peroxisome proliferator-activated receptor α and reduces body weight, TG, TC, liver injury markers, and inflammatory responses in animals with obesity induced by HFD. In addition, Wang *et al*[57] demonstrated the significant effects of *Ramulus mori* (Sangzhi) alkaloids (SZAs) on NAFLD mice. The results of research showed that SZAs reduced body weight, liver weight, blood glucose, blood lipids, and liver injury indicators in NAFLD mice, and improved metabolic disorders by downregulating key genes associated with liver lipid synthesis, such as *FASN* and *ACC*[57]. Our results demonstrated that HFD induced weight gain, increased liver index, elevated fat index, severe liver pathological injury, and significant lipid accumulation. In addition, HFD also led to changes in serum biochemical indexes, including increased levels of TG, TC and LDL-C, and decreased levels of HDL-C. After treatment with FLHZF, the weight of NAFLD mice decreased and the liver index returned to normal. FLHZF also significantly reversed liver pathological injury and lipid accumulation. FLHZF improved lipid indexes in serum, with decreased levels of TG and LDL-C, and increased level of HDL-C. FLHZF effectively restored the alignment of liver cells, reversed the elevation of liver injury indexes, and restored liver function as observed through HE staining and detection of liver injury indexes. These resulted confirmed that FLHZF administration significantly reduced lipid accumulation in animal and cellular models of NAFLD, but the specific mechanisms of this treatment was unclear.

With the growing acceptance of the "second strike" theory, numerous studies have demonstrated a close relationship between the pathogenesis of NAFLD and oxidative stress[58,59]. In NAFLD, lipid toxic substances, such as TG, can lead to production of ROS, activating oxidative stress and causing damage[60]. This oxidative damage can further mediate

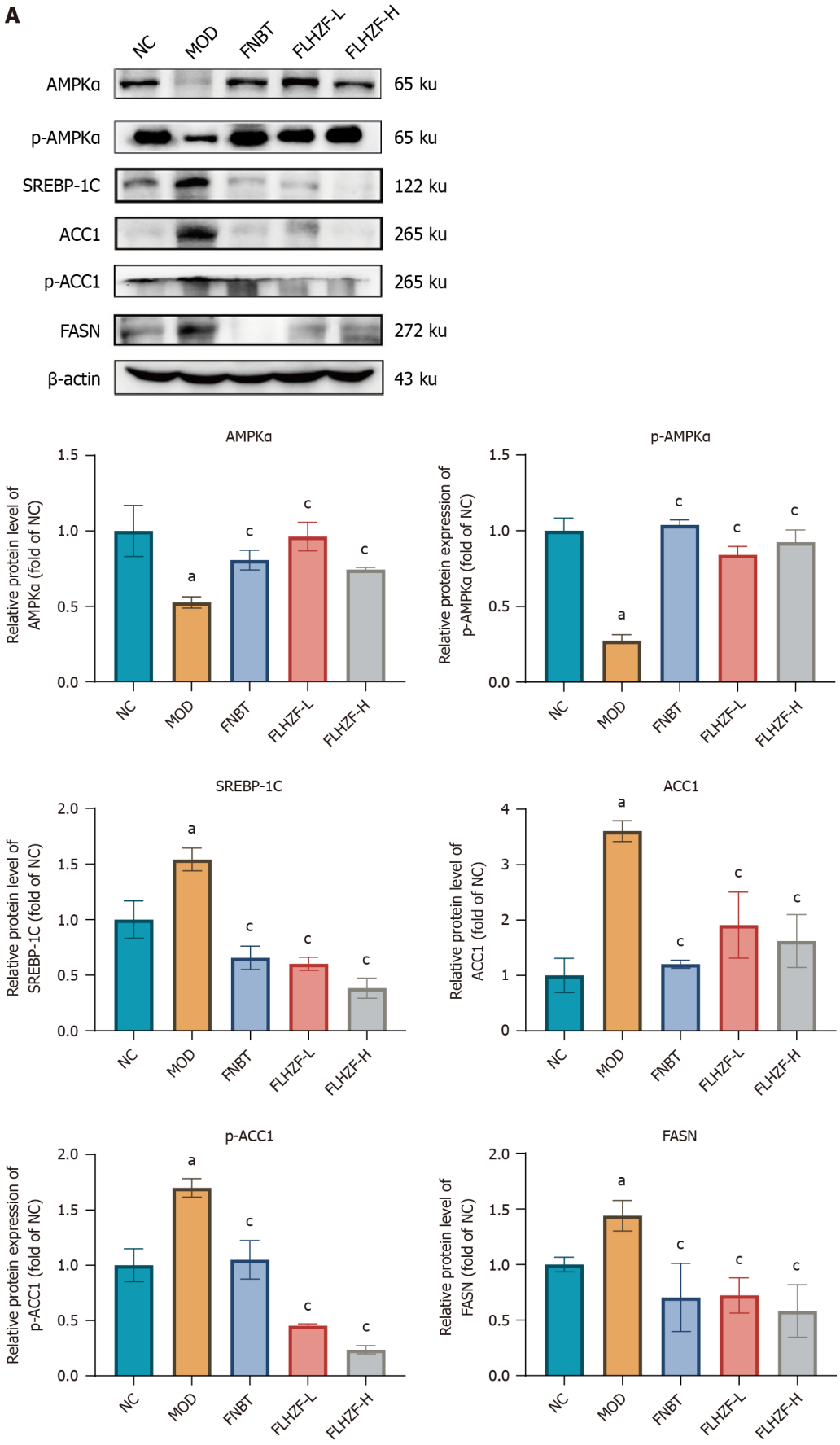
A
NC
MOD
FNBT
FLHZF-L
FLHZF-H
AMPKα
65 ku
p-AMPKα
65 ku
SREBP-1C
122 ku
ACC1
265 ku
p-ACC1
265 ku
FASN
272 ku
β-actin
43 ku
AMPKα
Relative protein level of AMPKα (fold of NC)
p-AMPKα
Relative protein expression of p-AMPKα (fold of NC)
SREBP-1C
Relative protein level of SREBP-1C (fold of NC)
ACC1
Relative protein level of ACC1 (fold of NC)
p-ACC1
Relative protein expression of p-ACC1 (fold of NC)
FASN
Relative protein level of FASN (fold of NC)

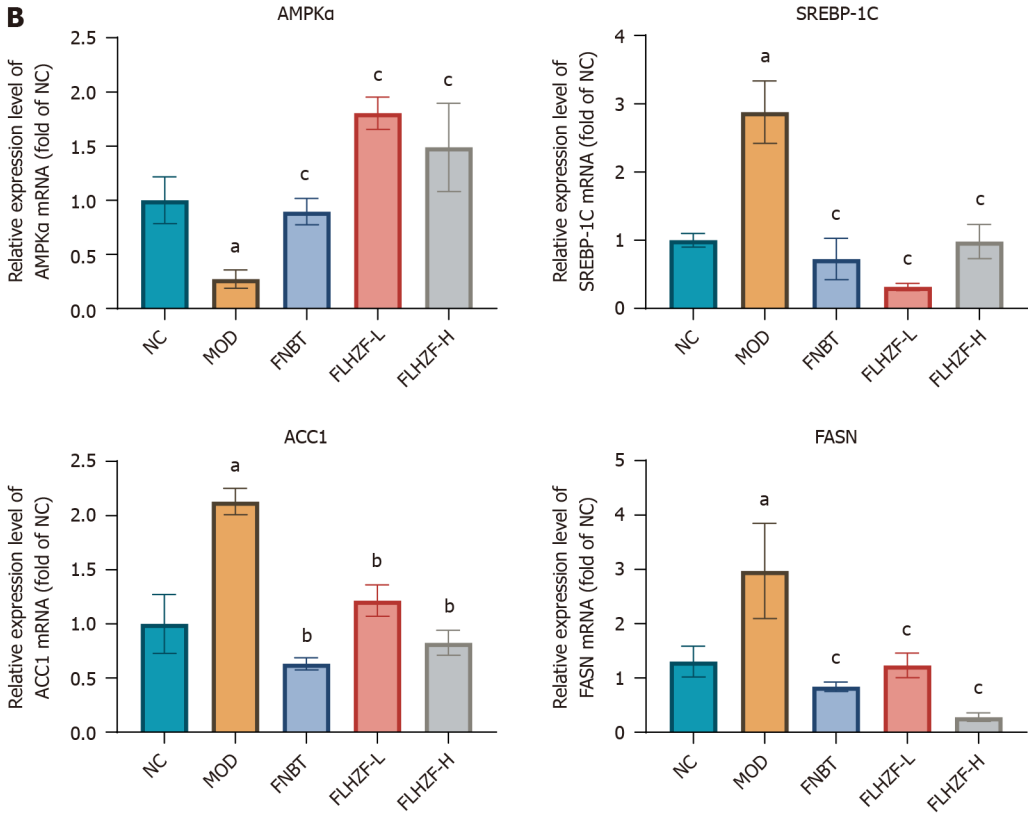

Figure 6 Fanlian Huazhuo Formula group regulated lipid synthesis signaling pathway *in vivo*. A: Protein expression levels of AMPKα, SREBP-1C, ACC1 and FASN in mice liver (n = 3); B: Relative mRNA expression levels of *AMPKα*, *SREBP-1C*, *ACC1* and *FASN* in mice liver (n = 3). Data are presented as mean ± SE. $^{a}P < 0.05$ *vs* NC group, $^{b}P < 0.01$ *vs* NC group, $^{c}P < 0.05$ *vs* MOD group. NC: Negative control group; MOD: Model group; FNBT: Fenofibrate group; FLHZF-L: Low dose of Fanlian Huazhuo Formula group; FLHZF-H: High dose of Fanlian Huazhuo Formula group.

mitochondrial dysfunction, resulting in hepatic lipid droplet overload and acceleration of hepatic steatosis[61,62]. SOD acts as the first line of defense against oxidative stress by converting superoxide anion radicals into H_2O_2 and oxygen. GSH-Px removes excess H_2O_2 by consuming GSH. MDA, the main product of lipid peroxidation damage, plays a crucial role in NAFLD progression. Therefore, increasing the abundance of SOD and GSH-Px and decreasing the level of MDA are important strategies for alleviating liver oxidative stress. Peng *et al*[55] demonstrated that Amides in *Z. Bungeanum* significantly improved oxidative stress in the liver of NAFLD mice by significantly increasing the abundance of SOD and GSH-Px, while decreasing the level of MDA. Hence, flow cytometry was used to detect the levels of ROS in HepG2 cells stimulated by FFA. The results showed that FLHZF reduced ROS accumulation in HepG2 cells stimulated by FFA, restoring it to normal levels. *In vivo*, FLHZF alleviated the abnormal changes in GSH-Px, MDA and SOD content in mouse liver caused by HFD. These findings revealed that FLHZF significantly reduced ROS accumulation and oxidative stress induced by the accumulation of lipid toxic substances in NAFLD, thereby reducing the accumulation of liver lipid droplets.

A previous study has demonstrated that the production of lipid peroxides induced by ROS can lead to a decrease in AMPKα activity[63]. AMPKα, in turn, regulates the key lipogenic proteins such as SREBP-1C, FASN, and ACC1, which play a crucial role in TG production[64,65]. Park *et al*[66] found that honey berry extraction increased expression of AMPKα and ACC but inhibited the levels of SREBP-1C and FASN, thereby reducing TG synthesis and lipid accumulation in NAFLD. Geethangili *et al*[67] validated that methyl bromide carboxylate increased expression of AMPKα phosphorylation and decreased mRNA expression levels of *ACC1, FASN* and *SREBP-1C*, resulting in reduced accumulation of lipid droplets and TG in liver cells induced by OA. These findings align with the *in vitro* and *in vivo* experimental results of our study. Notably, our study showed that FLHZF significantly increased expression of AMPKα and p-AMPKα, while inhibiting levels of SREBP-1C, ACC1, p-ACC1 and FASN. Consequently, FLHZF effectively reduced TG accumulation in NAFLD mice.

During the occurrence and development of NAFLD, the excessive production of ROS continuously attacks mitochondria, leading to mitochondrial decompensation, which in turn promotes lipid overload and inhibits autophagy [68]. Consequently, inhibition of autophagy results in significant accumulation of intracellular lipids, creating a self-perpetuating vicious cycle between lipid deposition and autophagy inhibition[68]. Therefore, activation of autophagy improves lipid deposition in NAFLD[69]. Jang *et al*[69] demonstrated that inhibiting Thrap3 activated AMPKα-mediated autophagy, thereby reducing the symptoms of NAFLD. Consistent with these results, FLHZF significantly increased protein expression of p-AMPKα and LC3A/B, as well as mRNA expression of *LC3A/B*. This activation of autophagy helped alleviate lipid accumulation in NAFLD.

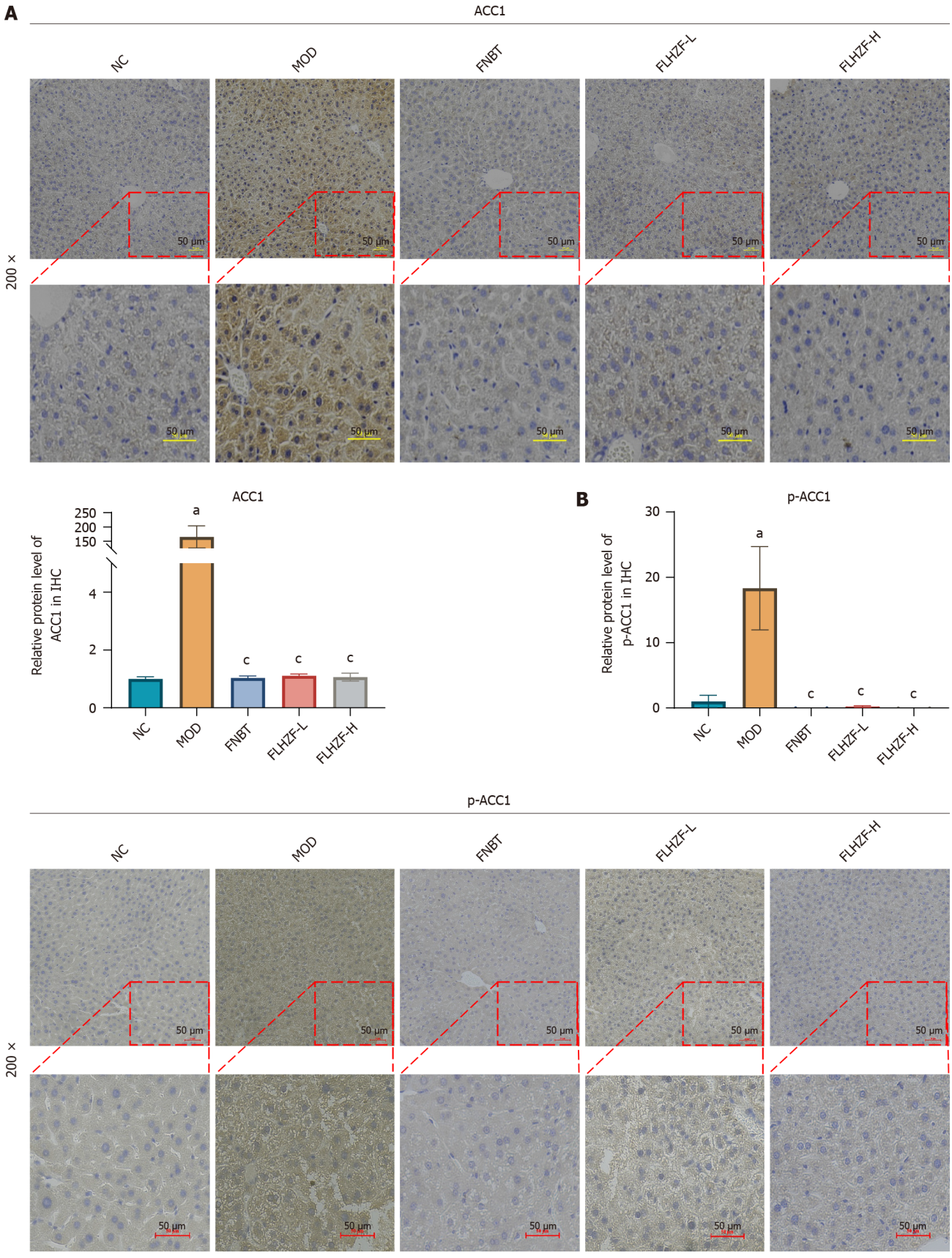
A
ACC1
NC
MOD
FNBT
FLHZF-L
FLHZF-H
200 ×
50 μm
ACC1
Relative protein level of ACC1 in IHC
250
200
150
4
2
0
a
c
c
c
NC
MOD
FNBT
FLHZF-L
FLHZF-H
B
p-ACC1
Relative protein level of p-ACC1 in IHC
30
20
10
0
a
c
c
c
NC
MOD
FNBT
FLHZF-L
FLHZF-H
p-ACC1
NC
MOD
FNBT
FLHZF-L
FLHZF-H
200 ×
50 μm

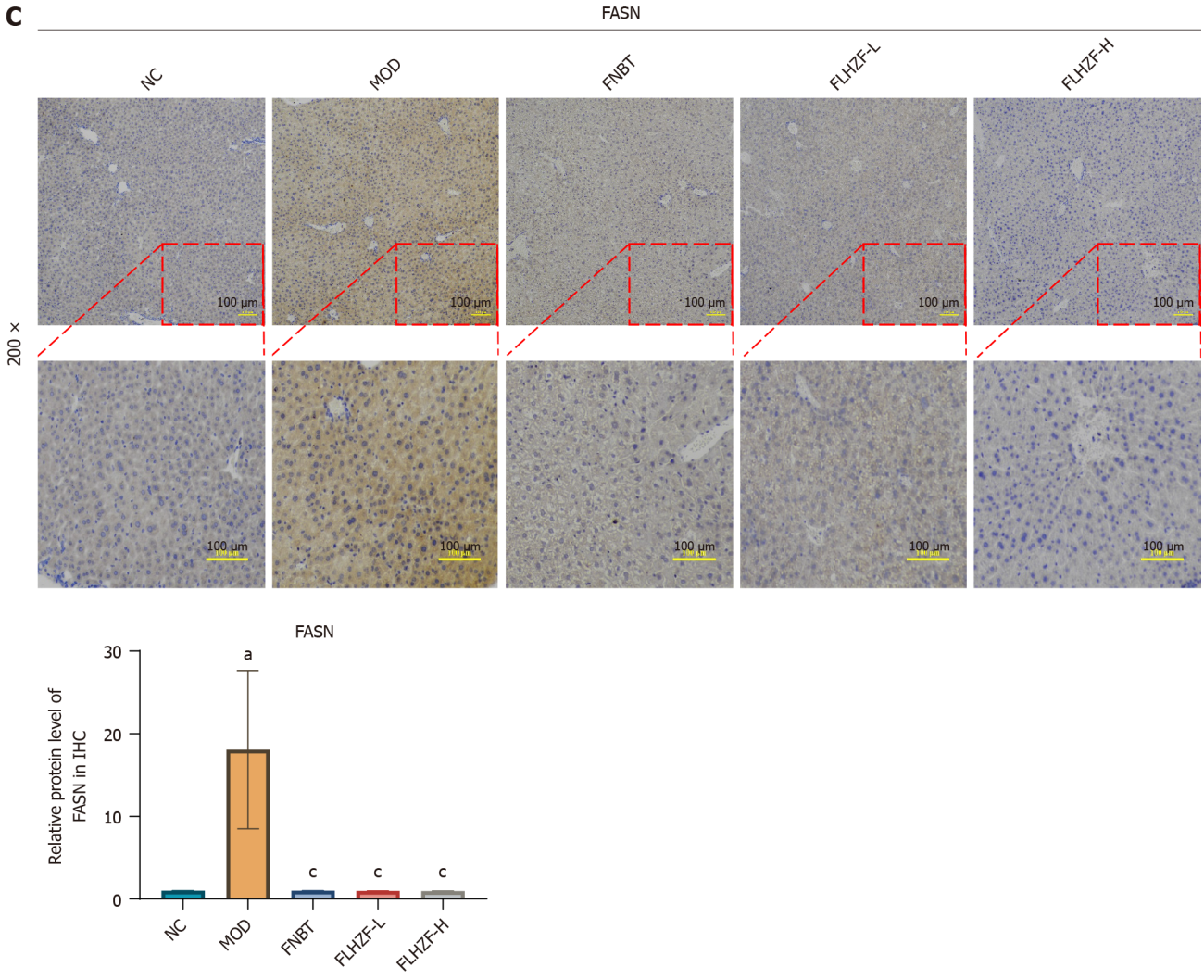

Figure 7 Fanlian Huazhuo Formula group regulated lipid synthesis signaling pathway *in vivo*. Representative images and quantification from immunohistochemistry for protein in mice liver, magnification 200 × (n = 3). A: ACC1; B: p-ACC1; C: FASN. Data are presented as mean ± SE. $^{a}P < 0.05$ *vs* NC group, $^{c}P < 0.05$ *vs* MOD group. NC: Negative control group; MOD: Model group; FNBT: Fenofibrate group; FLHZF-L: Low dose of Fanlian Huazhuo Formula group; FLHZF-H: High dose of Fanlian Huazhuo Formula group.

Studies have shown that apoptosis, a crucial aspect of NAFLD progression, is associated with oxidative stress and mitochondrial dysfunction[70,71]. Accumulation of ROS leads to changes in Bcl-2 family proteins (such as Bcl-2 and Bax), subsequently activating caspase-3 to promote apoptosis[72]. Bcl-2 and Bax play a significant role as regulatory factors in apoptosis, while cleaved caspase-3/9 induce apoptosis through mitochondrial-mediated pathways[73]. Han *et al*[70] demonstrated that Garcinia cambogia regulated expression of Bcl-2 and Bax, inhibiting apoptosis and reducing ROS production. In this study, we investigated the effects of FLHZF on the expression of Bcl-2, Bax and cleaved caspase-3. Our findings revealed that FLHZF significantly decreased protein and mRNA expression of Bax in NAFLD mice, increased protein and mRNA expressions of Bcl-2, and suppressed production of cleaved caspase-3. All these results suggest that FLHZF has the potential to inhibit ROS-mediated apoptosis.

The present study had some limitations. First, we did not assess the impact of FLHZF on gender, safety, and side effects. There may be gender differences in the effects of FLHZF, as well as potential safety and side effect issues. These aspects are worth in-depth study in future research, which will contribute to a more comprehensive understanding of the clinical application of FLHZF. Second, future research will add blinding procedures to ensure that the results are objective and not influenced by subjective factors. Lastly, exploration of the mechanism of action of FLHZF is not sufficient. Although our study has revealed some of the potential therapeutic effects of the formula, its underlying mechanism of action still needs to be elucidated. Future research will delve deeper into understanding the potential mechanisms of action of FLHZF.

CONCLUSION

Comparison of the therapeutic effects between the FLHZF-H and fenofibrate groups in the pharmacodynamic

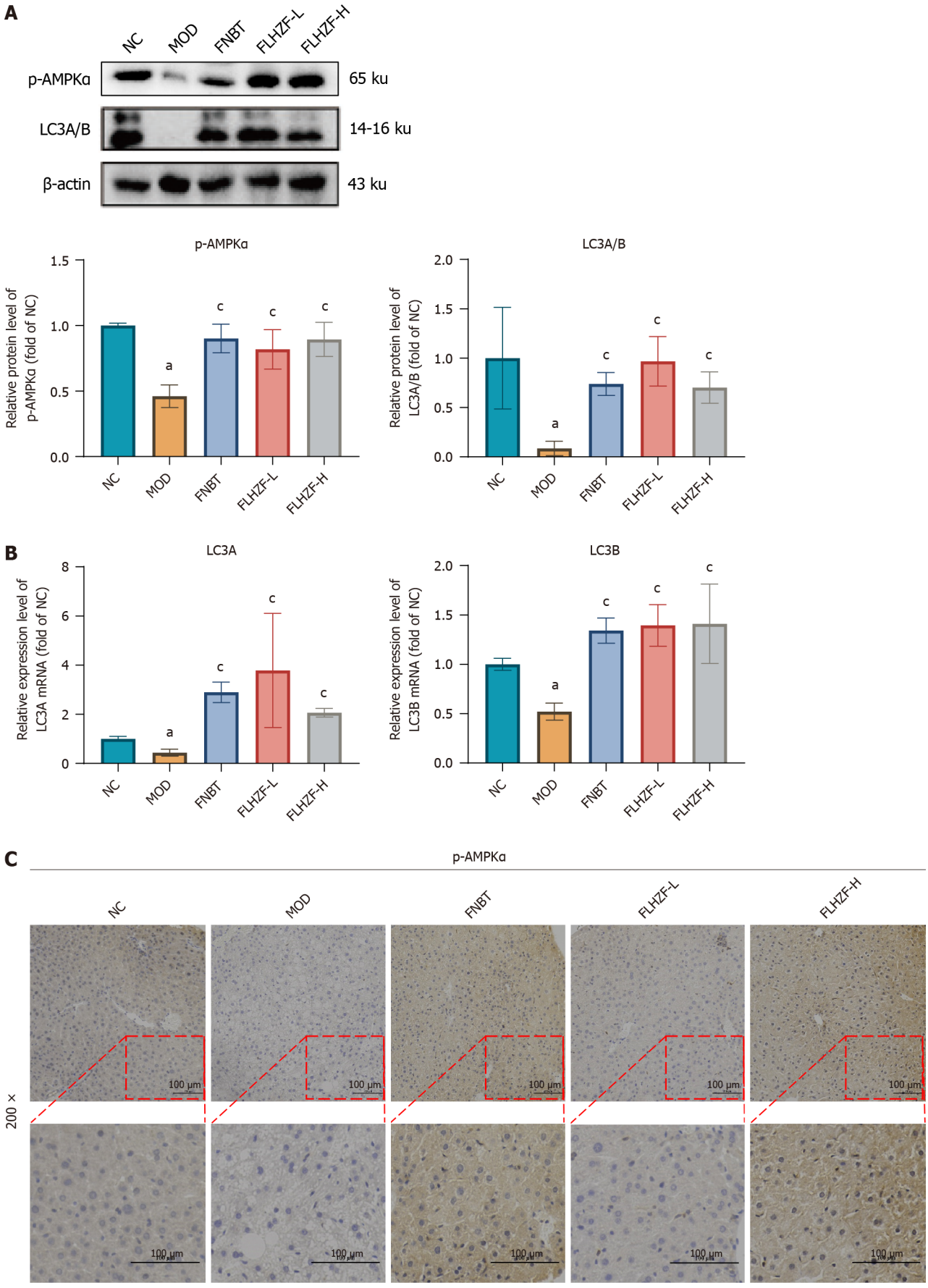
A
NC
MOD
FNBT
FLHZF-L
FLHZF-H
p-AMPKα
65 ku
LC3A/B
14-16 ku
β-actin
43 ku
p-AMPKα
Relative protein level of p-AMPKα (fold of NC)
LC3A/B
Relative protein level of LC3A/B (fold of NC)
B
LC3A
Relative expression level of LC3A mRNA (fold of NC)
LC3B
Relative expression level of LC3B mRNA (fold of NC)
C
p-AMPKα
200 ×
100 μm

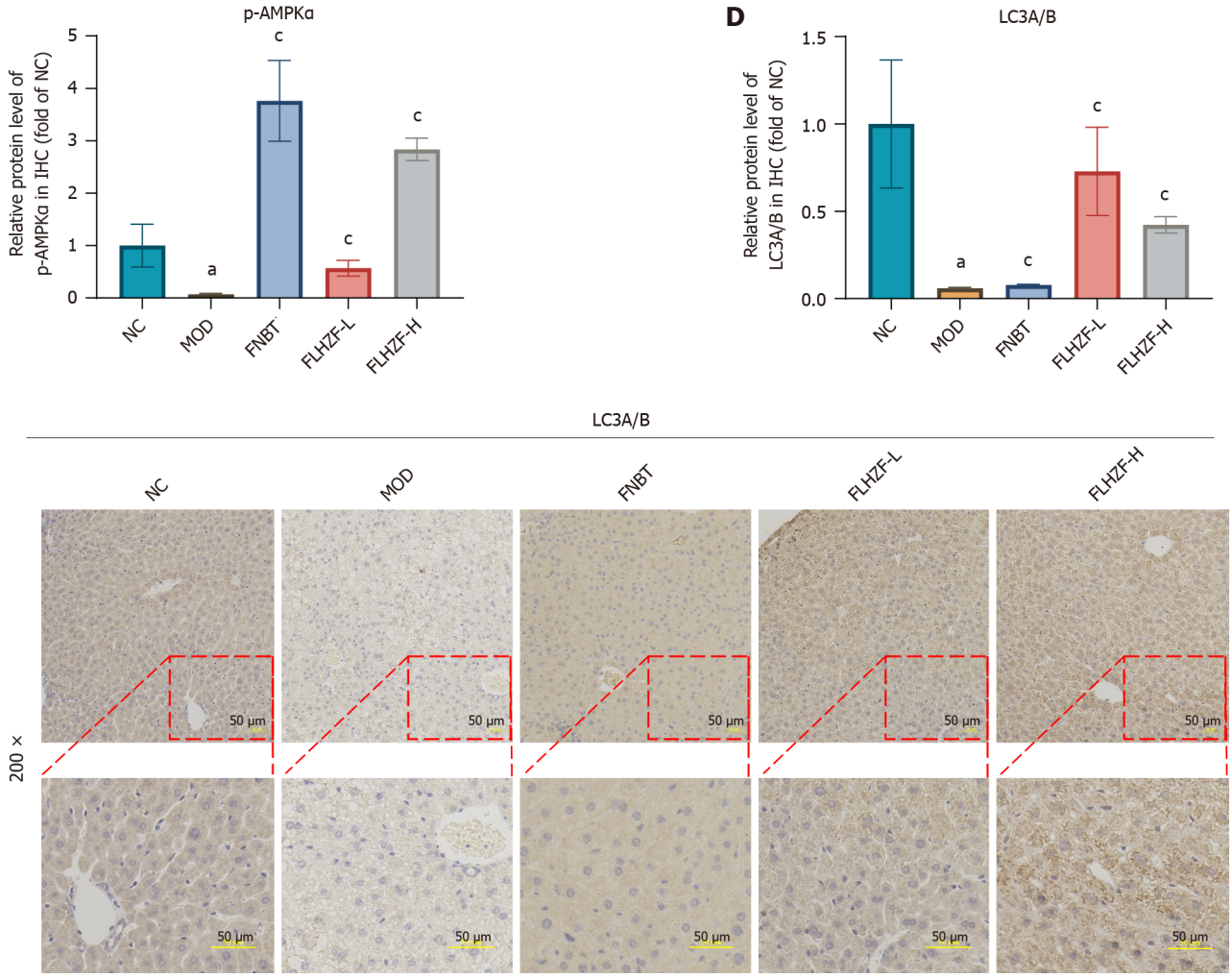

Figure 8 Fanlian Huazhuo Formula group regulated autophagy in mice induced by high-fat diet. A: Protein expression levels of LC3A/B and p-AMPKα in mice liver which were normalized by β-actin (n = 3); B: Relative mRNA expression levels of *LC3A* and *LC3B* in mice liver (n = 3); C: Representative images from immunohistochemistry for protein p-AMPKα in mice liver, magnification 200 × (n = 3); D: Representative images from immunohistochemistry for protein LC3A/B in mice liver, magnification 200 × (n = 3). Data are presented as mean ± SE. $^{a}P < 0.05$ *vs* NC group, $^{c}P < 0.05$ *vs* MOD group. NC: Negative control group; MOD: Model group; FNBT: Fenofibrate group; FLHZF-L: Low dose of Fanlian Huazhuo Formula group; FLHZF-H: High dose of Fanlian Huazhuo Formula group.

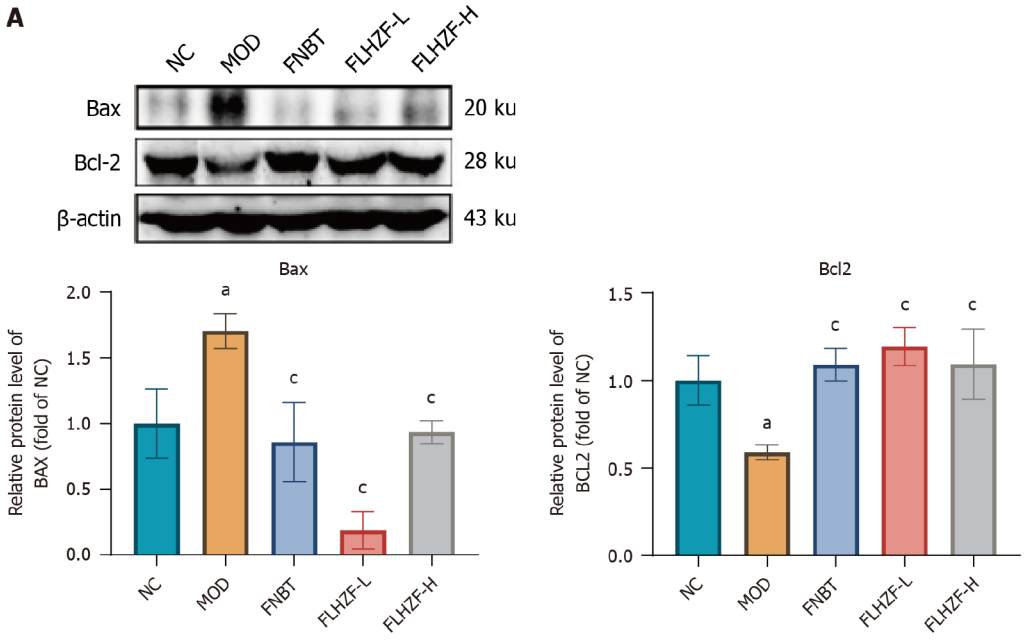

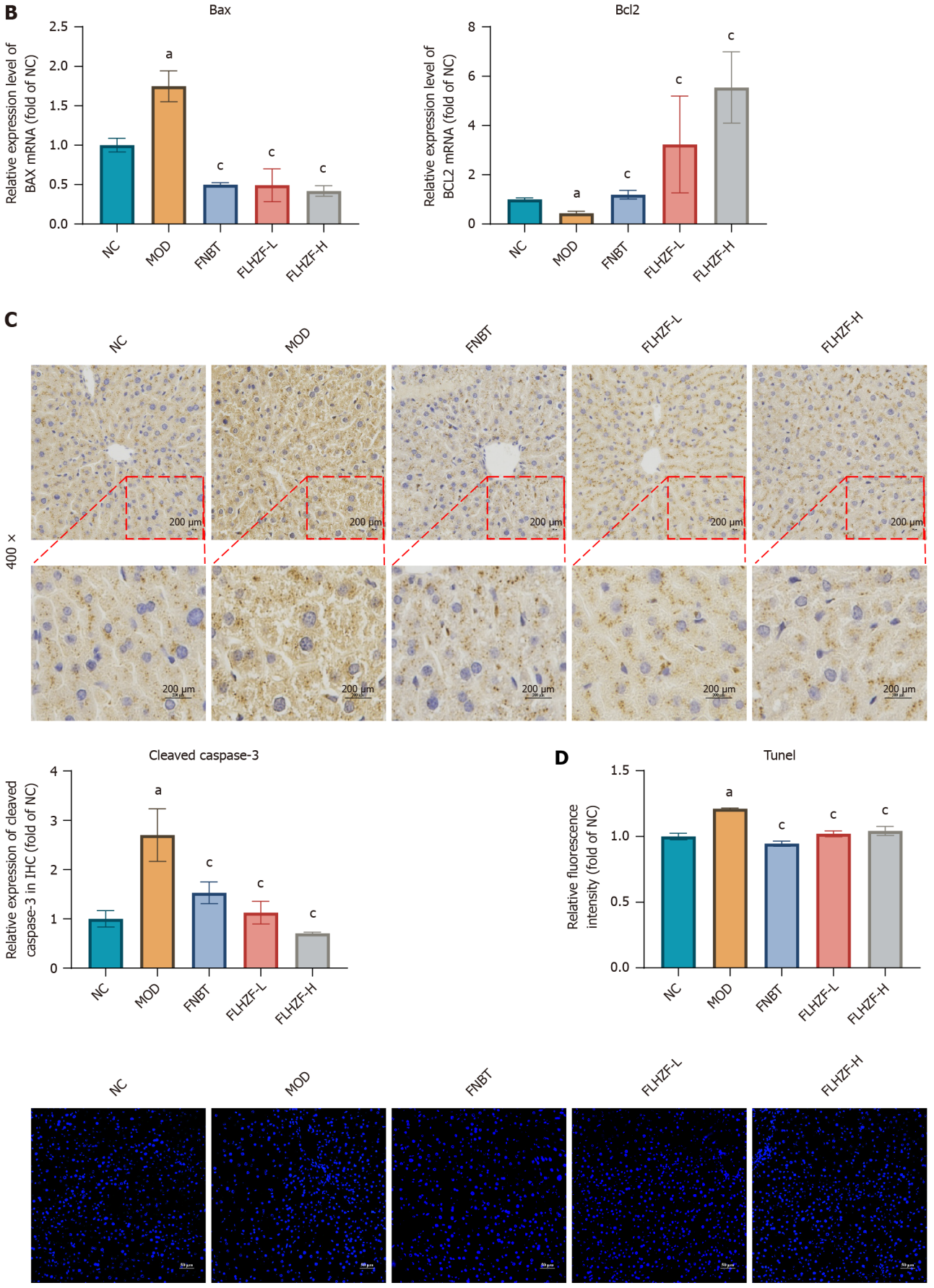
B
Bax
Relative expression level of BAX mRNA (fold of NC)
2.5
2.0
1.5
1.0
0.5
0.0
a
c
c
c
NC
MOD
FNBT
FLHZF-L
FLHZF-H
Bcl2
Relative expression level of BCL2 mRNA (fold of NC)
8
6
4
2
0
a
c
c
c
NC
MOD
FNBT
FLHZF-L
FLHZF-H
C
NC
MOD
FNBT
FLHZF-L
FLHZF-H
400 ×
200 μm
Cleaved caspase-3
Relative expression of cleaved caspase-3 in IHC (fold of NC)
4
3
2
1
0
a
c
c
c
NC
MOD
FNBT
FLHZF-L
FLHZF-H
D
Tunel
Relative fluorescence intensity (fold of NC)
1.5
1.0
0.5
0.0
a
c
c
c
NC
MOD
FNBT
FLHZF-L
FLHZF-H
NC
MOD
FNBT
FLHZF-L
FLHZF-H

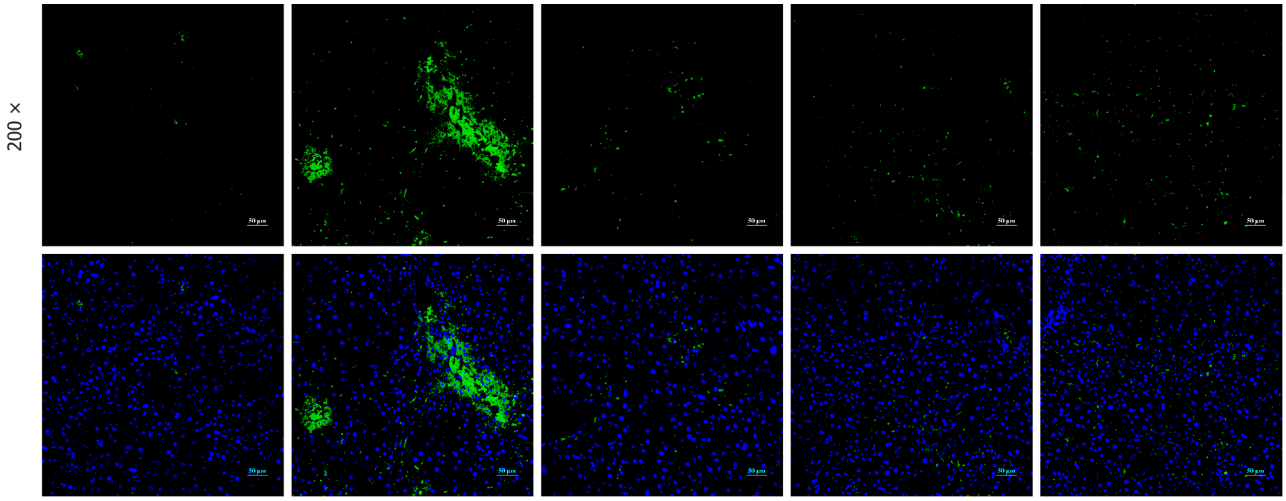

Figure 9 Fanlian Huazhuo Formula group reduced apoptosis in mice induced by high-fat diet. A: Protein expression levels of Bax and Bcl-2 in mice liver (n = 3); B: Hepatic mRNA expression levels of *Bax* and *Bcl-2* in mice liver (n = 3); C: Representative images and the quantification of immunohistochemistry for cleaved caspase-3 in mice liver, magnification 400 × (n = 3); D: Representative images and quantification of TUNEL staining of liver in mice, 200 × (n = 3). Data are presented as mean ± SE. $^{a}P < 0.05$ *vs* NC group, $^{c}P < 0.05$ *vs* MOD group. NC: Negative control group; MOD: Model group; FNBT: Fenofibrate group; FLHZF-L: Low dose of Fanlian Huazhuo Formula group; FLHZF-H: High dose of Fanlian Huazhuo Formula group.

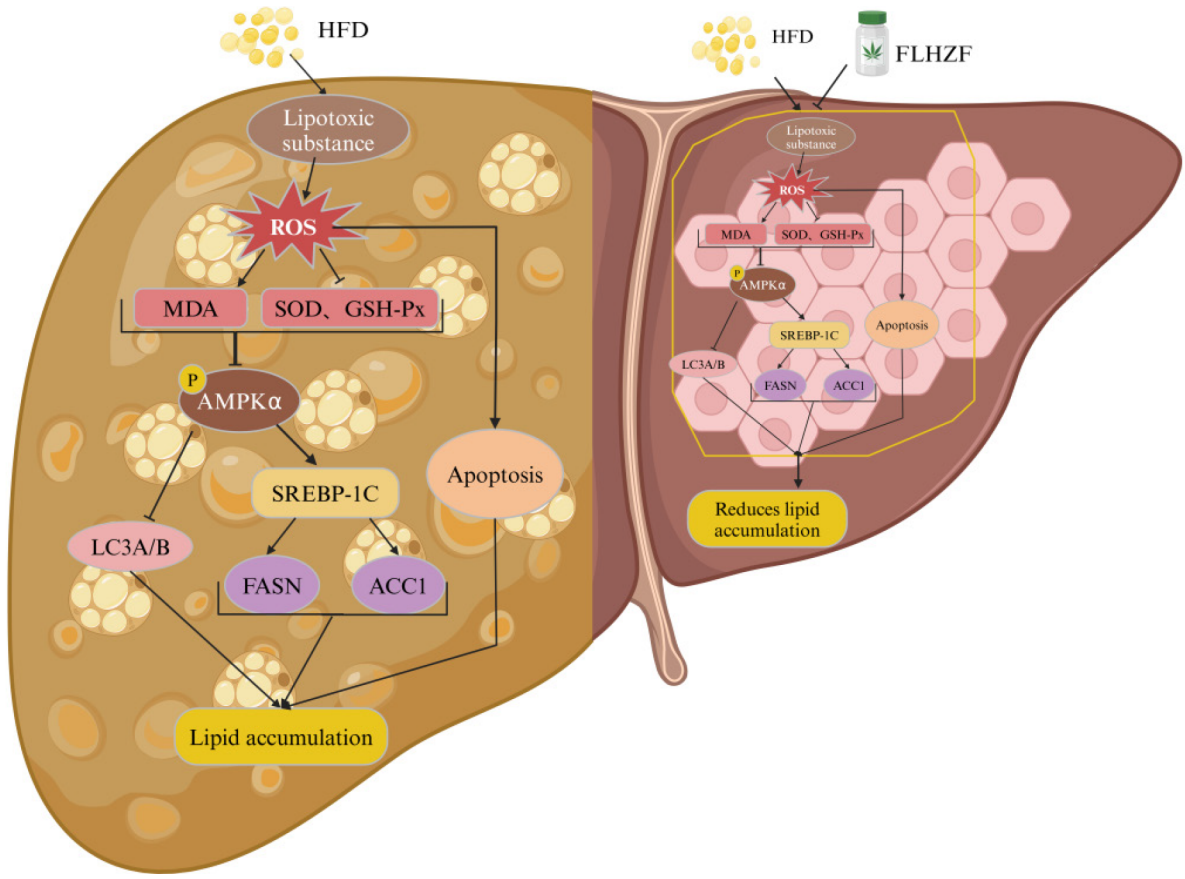

Figure 10 Diagrammatic representation of Fanlian Huazhuo Formula group protection against nonalcoholic fatty liver disease. FLHZF: Fanlian Huazhuo Formula; NAFLD: Nonalcoholic fatty liver disease; HFD: High-fat diet; MDA: Malondialdehyde; SOD: Superoxide dismutase: GSH-Px: Glutathione peroxidase. This figure was created by BioRender.com (Supplementary material).

experiments showed that, in terms of reducing weight gain, abdominal fat index and genital fat index, as well as serum ALT levels, the FLHZF-H group demonstrated better efficacy. In terms of reducing liver index, serum AST levels, NAS score, and the proportion of Oil Red O staining positive areas, there was no difference in the therapeutic effects between the FLHZF-H and fenofibrate groups. Therefore, FLHZF has superior therapeutic effects in multiple aspects, providing strong evidence for further research into its potential for treating NAFLD.

Our study suggests that FLHZF alleviates the build-up of lipid toxic substances in NAFLD through multiple mechanisms. These mechanisms (Figure 10) include reducing oxidative damage, activating autophagy and lipid synthesis signaling pathways associated with AMPKα, and inhibiting hepatocyte apoptosis. Our study broadens the application of FLHZF and offers an additional treatment option for NAFLD. In the future, metabolomics, will be used to study the specific effects of FLHZF in NAFLD. We aim to analyze the mechanisms by which FLHZF affects metabolic pathways and explore the relationship between these metabolic changes and metabolic diseases such as NAFLD, thereby offering new perspectives and strategies for their prevention and treatment.

FOOTNOTES

Author contributions: Niu MY and Dong GT designed the experiments, analyzed the data, and wrote the manuscript; Niu MY and Li Y conducted the experimental research; Luo Q, Cao L, Wang XM, Wang QW, Wang YT, Zhang Z, and Zhong XW provided the research software and experimental methods; Dai WB and Li LY contributed to the experimental design and financial support. All authors agree to be accountable for all aspects of work ensuring integrity and accuracy and approved the final manuscript. Niu MY and Dong GT contributed equally to this work as co-first authors. Corresponding authors Li LY and Dai WB, with their professional knowledge from different research fields, ensured the scientific authenticity of this study. They contributed to the development of the study plan and offered comprehensive support in securing study funding and acquiring resources. Li LY and Dai WB contributed equally to this work as co-corresponding authors.

Supported by Basic and Applied Basic Research Found of Guangdong Province, No. 2022A1515011307.

Institutional animal care and use committee statement: All procedures involving animals were reviewed and approved by the Institutional Animal Care and Use Committee of the Animal Ethics and Welfare Committee of Zhongshan Hospital of traditional Chinese Medicine (Protocol No. 2022042).

Conflict-of-interest statement: All the authors report no relevant conflicts of interest for this article

Data sharing statement: No additional data are available.

ARRIVE guidelines statement: The authors have read the ARRIVE guidelines, and the manuscript was prepared and revised according to the ARRIVE guidelines.

Country of origin: China

ORCID number: Wei-Bo Dai 0009-0001-3957-9043; Le-Yu Li 0009-0005-3721-1391.

S-Editor: Qu XL
L-Editor: A
P-Editor: Yuan YY

REFERENCES

1 **Younossi Z**, Tacke F, Arrese M, Chander Sharma B, Mostafa I, Bugianesi E, Wai-Sun Wong V, Yilmaz Y, George J, Fan J, Vos MB. Global Perspectives on Nonalcoholic Fatty Liver Disease and Nonalcoholic Steatohepatitis. *Hepatology* 2019; **69**: 2672-2682 [PMID: 30179269 DOI: 10.1002/hep.30251]

2 **Geng Y**, Faber KN, de Meijer VE, Blokzijl H, Moshage H. How does hepatic lipid accumulation lead to lipotoxicity in non-alcoholic fatty liver disease? *Hepatol Int* 2021; **15**: 21-35 [PMID: 33548031 DOI: 10.1007/s12072-020-10121-2]

3 **Younossi ZM**, Golabi P, Paik JM, Henry A, Van Dongen C, Henry L. The global epidemiology of nonalcoholic fatty liver disease (NAFLD) and nonalcoholic steatohepatitis (NASH): a systematic review. *Hepatology* 2023; **77**: 1335-1347 [PMID: 36626630 DOI: 10.1097/HEP.0000000000000004]

4 **Yu H**, Yan S, Jin M, Wei Y, Zhao L, Cheng J, Ding L, Feng H. Aescin can alleviate NAFLD through Keap1-Nrf2 by activating antioxidant and autophagy. *Phytomedicine* 2023; **113**: 154746 [PMID: 36905866 DOI: 10.1016/j.phymed.2023.154746]

5 **Li HY**, Peng ZG. Targeting lipophagy as a potential therapeutic strategy for nonalcoholic fatty liver disease. *Biochem Pharmacol* 2022; **197**: 114933 [PMID: 35093393 DOI: 10.1016/j.bcp.2022.114933]

6 **Marjot T**, Moolla A, Cobbold JF, Hodson L, Tomlinson JW. Nonalcoholic Fatty Liver Disease in Adults: Current Concepts in Etiology, Outcomes, and Management. *Endocr Rev* 2020; **41** [PMID: 31629366 DOI: 10.1210/endrev/bnz009]

7 **Teng T**, Qiu S, Zhao Y, Zhao S, Sun D, Hou L, Li Y, Zhou K, Yu X, Yang C, Li Y. Pathogenesis and Therapeutic Strategies Related to Non-Alcoholic Fatty Liver Disease. *Int J Mol Sci* 2022; **23** [PMID: 35887189 DOI: 10.3390/ijms23147841]

8 **Sun C**, Qiu C, Zhang Y, Yan M, Tan J, He J, Yang D, Wang D, Wu L. Lactiplantibacillus plantarum NKK20 Alleviates High-Fat-Diet-Induced Nonalcoholic Fatty Liver Disease in Mice through Regulating Bile Acid Anabolism. *Molecules* 2023; **28** [PMID: 37241783 DOI:

10.3390/molecules28104042]
9 **Ma X**, Qian H, Chen A, Ni HM, Ding WX. Perspectives on Mitochondria-ER and Mitochondria-Lipid Droplet Contact in Hepatocytes and Hepatic Lipid Metabolism. *Cells* 2021; **10** [PMID: 34571924 DOI: 10.3390/cells10092273]
10 **Zhang H**, Gao X, Chen P, Wang H. Protective Effects of Tiaoganquzhi Decoction in Treating inflammatory Injury of Nonalcoholic Fatty liver Disease by Promoting CGI-58 and Inhibiting Expression of NLRP3 Inflammasome. *Front Pharmacol* 2022; **13**: 851267 [PMID: 35586044 DOI: 10.3389/fphar.2022.851267]
11 **Li T**, Guo W, Zhou Z. Adipose Triglyceride Lipase in Hepatic Physiology and Pathophysiology. *Biomolecules* 2021; **12** [PMID: 35053204 DOI: 10.3390/biom12010057]
12 **Lian CY**, Zhai ZZ, Li ZF, Wang L. High fat diet-triggered non-alcoholic fatty liver disease: A review of proposed mechanisms. *Chem Biol Interact* 2020; **330**: 109199 [PMID: 32805210 DOI: 10.1016/j.cbi.2020.109199]
13 **Pourteymour S**, Drevon CA, Dalen KT, Norheim FA. Mechanisms Behind NAFLD: a System Genetics Perspective. *Curr Atheroscler Rep* 2023; **25**: 869-878 [PMID: 37812367 DOI: 10.1007/s11883-023-01158-3]
14 **Delli Bovi AP**, Marciano F, Mandato C, Siano MA, Savoia M, Vajro P. Oxidative Stress in Non-alcoholic Fatty Liver Disease. An Updated Mini Review. *Front Med (Lausanne)* 2021; **8**: 595371 [PMID: 33718398 DOI: 10.3389/fmed.2021.595371]
15 **Su LJ**, Zhang JH, Gomez H, Murugan R, Hong X, Xu D, Jiang F, Peng ZY. Reactive Oxygen Species-Induced Lipid Peroxidation in Apoptosis, Autophagy, and Ferroptosis. *Oxid Med Cell Longev* 2019; **2019**: 5080843 [PMID: 31737171 DOI: 10.1155/2019/5080843]
16 **Svegliati-Baroni G**, Pierantonelli I, Torquato P, Marinelli R, Ferreri C, Chatgilialoglu C, Bartolini D, Galli F. Lipidomic biomarkers and mechanisms of lipotoxicity in non-alcoholic fatty liver disease. *Free Radic Biol Med* 2019; **144**: 293-309 [PMID: 31152791 DOI: 10.1016/j.freeradbiomed.2019.05.029]
17 **Li H**, Ren J, Li Y, Wu Q, Wei J. Oxidative stress: The nexus of obesity and cognitive dysfunction in diabetes. *Front Endocrinol (Lausanne)* 2023; **14**: 1134025 [PMID: 37077347 DOI: 10.3389/fendo.2023.1134025]
18 **Zhao P**, Saltiel AR. From overnutrition to liver injury: AMP-activated protein kinase in nonalcoholic fatty liver diseases. *J Biol Chem* 2020; **295**: 12279-12289 [PMID: 32651233 DOI: 10.1074/jbc.REV120.011356]
19 **Moretti CH**, Schiffer TA, Li X, Weitzberg E, Carlström M, Lundberg JO. Germ-free mice are not protected against diet-induced obesity and metabolic dysfunction. *Acta Physiol (Oxf)* 2021; **231**: e13581 [PMID: 33222397 DOI: 10.1111/apha.13581]
20 **Lee SY**, Chung KS, Son SR, Lee SY, Jang DS, Lee JK, Kim HJ, Na CS, Lee SH, Lee KT. A Botanical Mixture Consisting of Inula japonica and Potentilla chinensis Relieves Obesity *via* the AMPK Signaling Pathway in 3T3-L1 Adipocytes and HFD-Fed Obese Mice. *Nutrients* 2022; **14** [PMID: 36145056 DOI: 10.3390/nu14183685]
21 **Fang C**, Pan J, Qu N, Lei Y, Han J, Zhang J, Han D. The AMPK pathway in fatty liver disease. *Front Physiol* 2022; **13**: 970292 [PMID: 36203933 DOI: 10.3389/fphys.2022.970292]
22 **Li H**, Xi Y, Xin X, Tian H, Hu Y. Gypenosides regulate farnesoid X receptor-mediated bile acid and lipid metabolism in a mouse model of non-alcoholic steatohepatitis. *Nutr Metab (Lond)* 2020; **17**: 34 [PMID: 32377219 DOI: 10.1186/s12986-020-00454-y]
23 **Lu MC**, Lee IT, Hong LZ, Ben-Arie E, Lin YH, Lin WT, Kao PY, Yang MD, Chan YC. Coffeeberry Activates the CaMKII/CREB/BDNF Pathway, Normalizes Autophagy and Apoptosis Signaling in Nonalcoholic Fatty Liver Rodent Model. *Nutrients* 2021; **13** [PMID: 34684653 DOI: 10.3390/nu13103652]
24 **Jian H**, Xu Q, Wang X, Liu Y, Miao S, Li Y, Mou T, Dong X, Zou X. Amino Acid and Fatty Acid Metabolism Disorders Trigger Oxidative Stress and Inflammatory Response in Excessive Dietary Valine-Induced NAFLD of Laying Hens. *Front Nutr* 2022; **9**: 849767 [PMID: 35495903 DOI: 10.3389/fnut.2022.849767]
25 **Wang Y**, Li J, Wang S, Pang Y, Liu P, Xie B, Dou S, Yang T, Liu X, Shi Y, Chen D. The hepatitis B virus promotes the progression of non-alcoholic fatty liver disease through incomplete autophagy. *Free Radic Biol Med* 2023; **204**: 326-336 [PMID: 37244371 DOI: 10.1016/j.freeradbiomed.2023.05.020]
26 **Ji L**, Li Q, He Y, Zhang X, Zhou Z, Gao Y, Fang M, Yu Z, Rodrigues RM, Gao Y, Li M. Therapeutic potential of traditional Chinese medicine for the treatment of NAFLD: A promising drug Potentilla discolor Bunge. *Acta Pharm Sin B* 2022; **12**: 3529-3547 [PMID: 36176915 DOI: 10.1016/j.apsb.2022.05.001]
27 **Xing QC**, Liu X, Li W, Chen YZ, Chen J. Sangguayin preparation prevents palmitate-induced apoptosis by suppressing endoplasmic reticulum stress and autophagy in db/db mice and MIN6 pancreatic β-cells. *Chin J Nat Med* 2020; **18**: 472-480 [PMID: 32503738 DOI: 10.1016/S1875-5364(20)30054-6]
28 **Beidokhti MN**, Eid HM, Villavicencio MLS, Jäger AK, Lobbens ES, Rasoanaivo PR, McNair LM, Haddad PS, Staerk D. Evaluation of the antidiabetic potential of Psidium guajava L. (Myrtaceae) using assays for α-glucosidase, α-amylase, muscle glucose uptake, liver glucose production, and triglyceride accumulation in adipocytes. *J Ethnopharmacol* 2020; **257**: 112877 [PMID: 32305639 DOI: 10.1016/j.jep.2020.112877]
29 **Vinayagam R**, Jayachandran M, Chung SSM, Xu B. Guava leaf inhibits hepatic gluconeogenesis and increases glycogen synthesis *via* AMPK/ACC signaling pathways in streptozotocin-induced diabetic rats. *Biomed Pharmacother* 2018; **103**: 1012-1017 [PMID: 29710658 DOI: 10.1016/j.biopha.2018.04.127]
30 **Feng X**, Li K, Tan F, Zhu M, Zhou J, Lai Y, Zeng L, Ye Y, Huang J, Wu X, Li S. Assessment of hepatoprotective potential of Radix Fici Hirtae on alcohol-induced liver injury in Kunming mice. *Biochem Biophys Rep* 2018; **16**: 69-73 [PMID: 30377670 DOI: 10.1016/j.bbrep.2018.10.003]
31 **Zhang R**, Zhang Q, Zhu S, Liu B, Liu F, Xu Y. Mulberry leaf (Morus alba L.): A review of its potential influences in mechanisms of action on metabolic diseases. *Pharmacol Res* 2022; **175**: 106029 [PMID: 34896248 DOI: 10.1016/j.phrs.2021.106029]
32 **Fan L**, Zhang C, Ai L, Wang L, Li L, Fan W, Li R, He L, Wu C, Huang Y. Traditional uses, botany, phytochemistry, pharmacology, separation and analysis technologies of Euonymus alatus (Thunb.) Siebold: A comprehensive review. *J Ethnopharmacol* 2020; **259**: 112942 [PMID: 32423879 DOI: 10.1016/j.jep.2020.112942]
33 **Gao SM**, Liu JS, Wang M, Cao TT, Qi YD, Zhang BG, Sun XB, Liu HT, Xiao PG. Traditional uses, phytochemistry, pharmacology and toxicology of Codonopsis: A review. *J Ethnopharmacol* 2018; **219**: 50-70 [PMID: 29501674 DOI: 10.1016/j.jep.2018.02.039]
34 **Shan Y**, Zhang S, Gao B, Liang S, Zhang H, Yu X, Zhao J, Ye L, Yang Q, Shang W. Adipose Tissue SIRT1 Regulates Insulin Sensitizing and Anti-Inflammatory Effects of Berberine. *Front Pharmacol* 2020; **11**: 591227 [PMID: 33390968 DOI: 10.3389/fphar.2020.591227]
35 **Wang J**, Wang L, Lou GH, Zeng HR, Hu J, Huang QW, Peng W, Yang XB. Coptidis Rhizoma: a comprehensive review of its traditional uses, botany, phytochemistry, pharmacology and toxicology. *Pharm Biol* 2019; **57**: 193-225 [PMID: 30963783 DOI: 10.1080/13880209.2019.1577466]

36 **Lin CC**, Li TC, Lai MM. Efficacy and safety of Monascus purpureus Went rice in subjects with hyperlipidemia. *Eur J Endocrinol* 2005; **153**: 679-686 [PMID: 16260426 DOI: 10.1530/eje.1.02012]

37 **Wang J**, Gao H, Ke D, Zuo G, Yang Y, Yamahara J, Li Y. Improvement of liquid fructose-induced adipose tissue insulin resistance by ginger treatment in rats is associated with suppression of adipose macrophage-related proinflammatory cytokines. *Evid Based Complement Alternat Med* 2013; **2013**: 590376 [PMID: 23533500 DOI: 10.1155/2013/590376]

38 **Kuo DH**, Yeh CH, Shieh PC, Cheng KC, Chen FA, Cheng JT. Effect of shanzha, a Chinese herbal product, on obesity and dyslipidemia in hamsters receiving high-fat diet. *J Ethnopharmacol* 2009; **124**: 544-550 [PMID: 19454308 DOI: 10.1016/j.jep.2009.05.005]

39 **Li L**, Huang G, Chen T, Lin H, Xu R, Cheng J, Hu Y, Dai W, Dong G. Fufang Fanshiliu Decoction Revealed the Antidiabetic Effect through Modulating Inflammatory Response and Gut Microbiota Composition. *Evid Based Complement Alternat Med* 2022; **2022**: 3255401 [PMID: 36262166 DOI: 10.1155/2022/3255401]

40 **Dai W**, Chen C, Dong G, Li G, Peng W, Liu X, Yang J, Li L, Xu R, Hu X. Alleviation of Fufang Fanshiliu decoction on type II diabetes mellitus by reducing insulin resistance: A comprehensive network prediction and experimental validation. *J Ethnopharmacol* 2022; **294**: 115338 [PMID: 35568115 DOI: 10.1016/j.jep.2022.115338]

41 **Li XX**, Lu XY, Zhang SJ, Chiu AP, Lo LH, Largaespada DA, Chen QB, Keng VW. Sodium tanshinone IIA sulfonate ameliorates hepatic steatosis by inhibiting lipogenesis and inflammation. *Biomed Pharmacother* 2019; **111**: 68-75 [PMID: 30576936 DOI: 10.1016/j.biopha.2018.12.019]

42 **Sheng D**, Zhao S, Gao L, Zheng H, Liu W, Hou J, Jin Y, Ye F, Zhao Q, Li R, Zhao N, Zhang L, Han Z, Wei L. BabaoDan attenuates high-fat diet-induced non-alcoholic fatty liver disease *via* activation of AMPK signaling. *Cell Biosci* 2019; **9**: 77 [PMID: 31548878 DOI: 10.1186/s13578-019-0339-2]

43 **Shen B**, Wang Y, Cheng J, Peng Y, Zhang Q, Li Z, Zhao L, Deng X, Feng H. Pterostilbene alleviated NAFLD *via* AMPK/mTOR signaling pathways and autophagy by promoting Nrf2. *Phytomedicine* 2023; **109**: 154561 [PMID: 36610156 DOI: 10.1016/j.phymed.2022.154561]

44 **Sheka AC**, Adeyi O, Thompson J, Hameed B, Crawford PA, Ikramuddin S. Nonalcoholic Steatohepatitis: A Review. *JAMA* 2020; **323**: 1175-1183 [PMID: 32207804 DOI: 10.1001/jama.2020.2298]

45 **Ok DP**, Ko K, Bae JY. Exercise without dietary changes alleviates nonalcoholic fatty liver disease without weight loss benefits. *Lipids Health Dis* 2018; **17**: 207 [PMID: 30172252 DOI: 10.1186/s12944-018-0852-z]

46 **Hye Khan MA**, Schmidt J, Stavniichuk A, Imig JD, Merk D. A dual farnesoid X receptor/soluble epoxide hydrolase modulator treats non-alcoholic steatohepatitis in mice. *Biochem Pharmacol* 2019; **166**: 212-221 [PMID: 31129048 DOI: 10.1016/j.bcp.2019.05.023]

47 **Ginsberg HN**, Packard CJ, Chapman MJ, Borén J, Aguilar-Salinas CA, Averna M, Ference BA, Gaudet D, Hegele RA, Kersten S, Lewis GF, Lichtenstein AH, Moulin P, Nordestgaard BG, Remaley AT, Staels B, Stroes ESG, Taskinen MR, Tokgözoğlu LS, Tybjaerg-Hansen A, Stock JK, Catapano AL. Triglyceride-rich lipoproteins and their remnants: metabolic insights, role in atherosclerotic cardiovascular disease, and emerging therapeutic strategies-a consensus statement from the European Atherosclerosis Society. *Eur Heart J* 2021; **42**: 4791-4806 [PMID: 34472586 DOI: 10.1093/eurheartj/ehab551]

48 **Luna-Castillo KP**, Olivares-Ochoa XC, Hernández-Ruiz RG, Llamas-Covarrubias IM, Rodríguez-Reyes SC, Betancourt-Núñez A, Vizmanos B, Martínez-López E, Muñoz-Valle JF, Márquez-Sandoval F, López-Quintero A. The Effect of Dietary Interventions on Hypertriglyceridemia: From Public Health to Molecular Nutrition Evidence. *Nutrients* 2022; **14** [PMID: 35268076 DOI: 10.3390/nu14051104]

49 **Feldman F**, Koudoufio M, El-Jalbout R, Sauvé MF, Ahmarani L, Sané AT, Ould-Chikh NE, N'Timbane T, Patey N, Desjardins Y, Stintzi A, Spahis S, Levy E. Cranberry Proanthocyanidins as a Therapeutic Strategy to Curb Metabolic Syndrome and Fatty Liver-Associated Disorders. *Antioxidants (Basel)* 2022; **12** [PMID: 36670951 DOI: 10.3390/antiox12010090]

50 **Asghari S**, Hamedi-Shahraki S, Amirkhizi F. Systemic redox imbalance in patients with nonalcoholic fatty liver disease. *Eur J Clin Invest* 2020; **50**: e13211 [PMID: 32017057 DOI: 10.1111/eci.13211]

51 **Abulikemu A**, Zhao X, Xu H, Li Y, Ma R, Yao Q, Wang J, Sun Z, Li Y, Guo C. Silica nanoparticles aggravated the metabolic associated fatty liver disease through disturbed amino acid and lipid metabolisms-mediated oxidative stress. *Redox Biol* 2023; **59**: 102569 [PMID: 36512914 DOI: 10.1016/j.redox.2022.102569]

52 **Wei Q**, Zhou B, Yang G, Hu W, Zhang L, Liu R, Li M, Wang K, Gu HF, Guan Y, Zhu Z, Zheng H, Peng J, Li L. JAZF1 ameliorates age and diet-associated hepatic steatosis through SREBP-1c -dependent mechanism. *Cell Death Dis* 2018; **9**: 859 [PMID: 30154417 DOI: 10.1038/s41419-018-0923-0]

53 **Wang Y**, Chen C, Chen J, Sang T, Peng H, Lin X, Zhao Q, Chen S, Eling T, Wang X. Overexpression of NAG-1/GDF15 prevents hepatic steatosis through inhibiting oxidative stress-mediated dsDNA release and AIM2 inflammasome activation. *Redox Biol* 2022; **52**: 102322 [PMID: 35504134 DOI: 10.1016/j.redox.2022.102322]

54 **Zhang J**, Ma X, Fan D. Ginsenoside CK ameliorates hepatic lipid accumulation *via* activating the LKB1/AMPK pathway in vitro and in vivo. *Food Funct* 2022; **13**: 1153-1167 [PMID: 35018944 DOI: 10.1039/d1fo03026d]

55 **Peng W**, He CX, Li RL, Qian D, Wang LY, Chen WW, Zhang Q, Wu CJ. Zanthoxylum bungeanum amides ameliorates nonalcoholic fatty liver *via* regulating gut microbiota and activating AMPK/Nrf2 signaling. *J Ethnopharmacol* 2024; **318**: 116848 [PMID: 37423515 DOI: 10.1016/j.jep.2023.116848]

56 **Tovar R**, de Ceglia M, Ubaldi M, Rodríguez-Pozo M, Soverchia L, Cifani C, Rojo G, Gavito A, Hernandez-Folgado L, Jagerovic N, Ciccocioppo R, Baixeras E, Rodríguez de Fonseca F, Decara J. Administration of Linoleoylethanolamide Reduced Weight Gain, Dyslipidemia, and Inflammation Associated with High-Fat-Diet-Induced Obesity. *Nutrients* 2023; **15** [PMID: 37892524 DOI: 10.3390/nu15204448]

57 **Wang F**, Xu SJ, Ye F, Zhang B, Sun XB. Integration of Transcriptomics and Lipidomics Profiling to Reveal the Therapeutic Mechanism Underlying Ramulus mori (Sangzhi) Alkaloids for the Treatment of Liver Lipid Metabolic Disturbance in High-Fat-Diet/Streptozotocin-Induced Diabetic Mice. *Nutrients* 2023; **15** [PMID: 37764698 DOI: 10.3390/nu15183914]

58 **Chen Z**, Tian R, She Z, Cai J, Li H. Role of oxidative stress in the pathogenesis of nonalcoholic fatty liver disease. *Free Radic Biol Med* 2020; **152**: 116-141 [PMID: 32156524 DOI: 10.1016/j.freeradbiomed.2020.02.025]

59 **Hong T**, Chen Y, Li X, Lu Y. The Role and Mechanism of Oxidative Stress and Nuclear Receptors in the Development of NAFLD. *Oxid Med Cell Longev* 2021; **2021**: 6889533 [PMID: 34745420 DOI: 10.1155/2021/6889533]

60 **Zhang R**, Chu K, Zhao N, Wu J, Ma L, Zhu C, Chen X, Wei G, Liao M. Corilagin Alleviates Nonalcoholic Fatty Liver Disease in High-Fat Diet-Induced C57BL/6 Mice by Ameliorating Oxidative Stress and Restoring Autophagic Flux. *Front Pharmacol* 2019; **10**: 1693 [PMID: 32116684 DOI: 10.3389/fphar.2019.01693]

61 **Arroyave-Ospina JC**, Wu Z, Geng Y, Moshage H. Role of Oxidative Stress in the Pathogenesis of Non-Alcoholic Fatty Liver Disease: Implications for Prevention and Therapy. *Antioxidants (Basel)* 2021; **10** [PMID: 33530432 DOI: 10.3390/antiox10020174]

62 **Mohamed J**, Nazratun Nafizah AH, Zariyantey AH, Budin SB. Mechanisms of Diabetes-Induced Liver Damage: The role of oxidative stress and inflammation. *Sultan Qaboos Univ Med J* 2016; **16**: e132-e141 [PMID: 27226903 DOI: 10.18295/squmj.2016.16.02.002]

63 **Liang L**, Ye S, Jiang R, Zhou X, Zhou J, Meng S. Liensinine alleviates high fat diet (HFD)-induced non-alcoholic fatty liver disease (NAFLD) through suppressing oxidative stress and inflammation *via* regulating TAK1/AMPK signaling. *Int Immunopharmacol* 2022; **104**: 108306 [PMID: 34999396 DOI: 10.1016/j.intimp.2021.108306]

64 **Fang K**, Wu F, Chen G, Dong H, Li J, Zhao Y, Xu L, Zou X, Lu F. Diosgenin ameliorates palmitic acid-induced lipid accumulation *via* AMPK/ACC/CPT-1A and SREBP-1c/FAS signaling pathways in LO2 cells. *BMC Complement Altern Med* 2019; **19**: 255 [PMID: 31519174 DOI: 10.1186/s12906-019-2671-9]

65 **Yin X**, Liu Z, Wang J. Tetrahydropalmatine ameliorates hepatic steatosis in nonalcoholic fatty liver disease by switching lipid metabolism *via* AMPK-SREBP-1c-Sirt1 signaling axis. *Phytomedicine* 2023; **119**: 155005 [PMID: 37562090 DOI: 10.1016/j.phymed.2023.155005]

66 **Park M**, Yoo JH, Lee YS, Lee HJ. Lonicera caerulea Extract Attenuates Non-Alcoholic Fatty Liver Disease in Free Fatty Acid-Induced HepG2 Hepatocytes and in High Fat Diet-Fed Mice. *Nutrients* 2019; **11** [PMID: 30813654 DOI: 10.3390/nu11030494]

67 **Geethangili M**, Lin CW, Mersmann HJ, Ding ST. Methyl Brevifolincarboxylate Attenuates Free Fatty Acid-Induced Lipid Metabolism and Inflammation in Hepatocytes through AMPK/NF-κB Signaling Pathway. *Int J Mol Sci* 2021; **22** [PMID: 34576229 DOI: 10.3390/ijms221810062]

68 **Zhang D**, Zhang Y, Wang Z, Lei L. Thymoquinone attenuates hepatic lipid accumulation by inducing autophagy *via* AMPK/mTOR/ULK1-dependent pathway in nonalcoholic fatty liver disease. *Phytother Res* 2023; **37**: 781-797 [PMID: 36479746 DOI: 10.1002/ptr.7662]

69 **Jang HJ**, Lee YH, Dao T, Jo Y, Khim KW, Eom HJ, Lee JE, Song YJ, Choi SS, Park K, Ji H, Chae YC, Myung K, Kim H, Ryu D, Park NH, Park SH, Choi JH. Thrap3 promotes nonalcoholic fatty liver disease by suppressing AMPK-mediated autophagy. *Exp Mol Med* 2023; **55**: 1720-1733 [PMID: 37524868 DOI: 10.1038/s12276-023-01047-4]

70 **Han JH**, Park MH, Myung CS. Garcinia cambogia Ameliorates Non-Alcoholic Fatty Liver Disease by Inhibiting Oxidative Stress-Mediated Steatosis and Apoptosis through NRF2-ARE Activation. *Antioxidants (Basel)* 2021; **10** [PMID: 34439474 DOI: 10.3390/antiox10081226]

71 **Zhang L**, Xie Z, Yu H, Du H, Wang X, Cai J, Qiu Y, Chen R, Jiang X, Liu Z, Li Y, Chen T. TLR2 inhibition ameliorates the amplification effect of LPS on lipid accumulation and lipotoxicity in hepatic cells. *Ann Transl Med* 2021; **9**: 1429 [PMID: 34733981 DOI: 10.21037/atm-21-4012]

72 **Wu D**, Liu Z, Wang Y, Zhang Q, Li J, Zhong P, Xie Z, Ji A, Li Y. Epigallocatechin-3-Gallate Alleviates High-Fat Diet-Induced Nonalcoholic Fatty Liver Disease *via* Inhibition of Apoptosis and Promotion of Autophagy through the ROS/MAPK Signaling Pathway. *Oxid Med Cell Longev* 2021; **2021**: 5599997 [PMID: 33953830 DOI: 10.1155/2021/5599997]

73 **Ji X**, Ma Q, Wang X, Ming H, Bao G, Fu M, Wei C. Digeda-4 decoction and its disassembled prescriptions improve dyslipidemia and apoptosis by regulating AMPK/SIRT1 pathway on tyloxapol-induced nonalcoholic fatty liver disease in mice. *J Ethnopharmacol* 2023; **317**: 116827 [PMID: 37348794 DOI: 10.1016/j.jep.2023.116827]

Published by **Baishideng Publishing Group Inc**
7041 Koll Center Parkway, Suite 160, Pleasanton, CA 94566, USA
Telephone: +1-925-3991568
E-mail: office@baishideng.com
Help Desk: https://www.f6publishing.com/helpdesk
https://www.wjgnet.com